Local adaptation drives thermoregulation in tropical rainforest trees

Kali Middleby[1], Rebecca Jordan[1], Alexander W. Cheesman[1], Maurizio Rossetto[1], Martin F. Breed[1], Darren M. Crayn[1], and Lucas A. Cernusak[1]

[1]Affiliation not available

November 15, 2024

Abstract

Globally, the increasing frequency of heatwaves and droughts are impacting tropical forests, which are vital for maintaining biodiversity, carbon sequestration and climate regulation. But vulnerability to warming may vary between and within species due to phenotypic divergence. Leaf functional trait variation is known to affect leaf operating temperatures – a phenomenon termed 'limited homeothermy' when it helps avoid lethal temperatures in warmer conditions. Yet, evidence of this purported thermoregulatory ability and the relative roles of acclimation or adaptation remain limited.

Here we measured photosynthetic heat tolerance and leaf thermal traits of three, co-occurring tropical rainforest trees across a wide thermal gradient in the Australian Wet Tropics. We used observed leaf traits to predict leaf-to-air temperature differences ($[?]T_{trait}$) and combined this with genotypic and environmental data from field collections and glasshouse experiments to assess evidence for intraspecific adaptive selection across the landscape.

Intraspecific trait variation led to enhanced leaf cooling (lower or more negative $[?]T_{trait}$) and partial maintenance of modelled thermal safety margins in warmer sites for *Darlingia darlingiana* and *Elaeocarpus grandis,* but not *Cardwellia sublimis.* Genomic signals of selection were detected in all three species, with adaptive genomic variation associated with climate for *D. darlingiana* and *E. grandis,* but edaphic factors for *C. sublimis.* Additionally, *E. grandis* seedlings from different provenances grown under contrasting temperature and humidity regimes showed clines in $[?]T_{trait}$ variation related to mean annual temperature of origin but not treatment environment, despite individual traits acclimating to treatments.

Our work implicates local adaptation to climate as a driver of intraspecific variation in leaf thermoregulatory traits, supporting limited homeothermy in these key tropical rainforest tree species. Our results highlight how leaf energy balance modelling can be combined with ecological genomics to better understand the strategies plants use to cope with rising temperatures.

Introduction

Global warming is rapidly increasing temperatures, raising concerns about the ability of species to persist (IPCC, 2022). Tropical forest trees, vital for maintaining biodiversity, carbon sequestration and water cycling (Mitchard, 2018), may be particularly vulnerable due to their evolution under relatively stable thermal environments (Trew & Maclean, 2021). However, populations from across climate gradients in the landscape may be found to respond differently to environmental change due to plasticity or local adaptation

(Barton et al., 2020; Halbritter et al., 2018; Leites & Garzón, 2023; Matesanz & Ramirez-Valiente, 2019; Muehleisen et al., 2020). While local adaptation can enhance fitness under stable conditions, it may inhibit future persistence if climate change creates a mismatch between the historic conditions a population is adapted to and the new environment (Jordan et al., 2024). Therefore, understanding how tropical trees have adapted to temperature is crucial for evaluating their resilience to global warming and informing effective management strategies.

Plants have evolved various mechanisms to cope with heat stress and maintain physiological function, such as altering leaf-level biochemistry to increase their photosynthetic heat tolerance (Geange et al., 2021; Middleby, Cheesman, & Cernusak, 2024). Such adjustments help prevent leaf senescence and maintain carbon uptake during heatwaves (Drake et al., 2018). However, recent studies indicate that this may be insufficient to preserve thermal safety margins in warmer environments (Kullberg et al., 2023; Perez & Feeley, 2020). As such, species or populations near their thermal limits, such as those found in lowland tropical forests, may be particularly vulnerable to even small temperature increases in the coming decades (Araujo et al., 2021; Doughty et al., 2023; Pau et al., 2018).

Plants can also cope with thermal stress by avoiding high temperatures through morphological and physiological trait variations that influence leaf energy balance (Michaletz et al., 2015). Traits like leaf width, absorptance, leaf angle, and stomatal conductance interact with the canopy microclimate to influence the fluxes of sensible and latent heat and the interception of radiation (Campbell & Norman, 1998; Jones, 2013). This leads to significant differences between leaf and air temperatures ([?]T = T_{leaf}-T_{air}), with variations +-20degC observed due to differences in water use (Fauset et al., 2018), leaf morphology (Leigh et al., 2017), and canopy architecture (Leuzinger & Korner, 2007; Woods et al., 2018). Given the importance of maintaining T_{leaf} within safe operating limits, it is hypothesised that traits influencing [?]T may undergo selection for enhanced leaf cooling in warmer environments (Mahan & Upchurch, 1988; Michaletz et al., 2015). While such thermoregulation has been noted across different ecosystems (Guo et al., 2023; Kitudom et al., 2022), studies within species are limited (Kullberg et al., 2023), and few have explored the relative roles of phenotypic plasticity and ecotypic variation (Middleby, Cheesman, Hopkinson, et al., 2024).

Across species distributions, temperature often varies with other environmental factors such as precipitation, humidity, and soil nutrients, which can impact trait trade-offs (Rolhauser et al., 2021) and [?]T. For instance, a common garden trial comparing T_{leaf} in upland and lowland provenances of tropical rainforest species showed varying provenance effects on T_{leaf} (Middleby, Cheesman, Hopkinson, et al., 2024). This variation might result from competing pressures such as vapour pressure deficit (VPD) and temperature on stomatal conductance (Middleby, Cheesman, & Cernusak, 2024). While plant gas exchange must balance carbon uptake and water use, leaf cooling is also crucial (Blonder et al., 2023). If temperature strongly drives selection, traits that keep T_{leaf} within safe limits may be favoured in warmer regions.

Understanding local adaptation to temperature in tropical trees is essential for predicting their future vulnerability, and guiding revegetation efforts to match provenance with future site conditions (Breed et al., 2013; Jordan et al., 2024). While common garden and reciprocal transplant experiments are ideal for studying local adaptation, they are resource-intensive (Sork et al., 2013), especially in remote areas. Population and ecological genomic methods, such as genotype-environment (GEA) and genotype-phenotype (GPA) associations, offer complementary insights into adaptative potential without extensive field trials (Arab et al., 2020; Breed et al., 2019; Shryock et al., 2021; Steane et al., 2014; Weigand & Leese, 2018).

Here we investigated climate adaptation in three tropical tree species by examining intraspecific variation in leaf thermoregulation. We hypothesized that traits associated with leaf cooling are under selection. This hypothesis predicts that:

1. Within species, individuals exposed to warmer temperatures show coordination of leaf thermal traits that enhance leaf cooling.
2. Adaptive genetic variation associated with leaf thermal traits is positively correlated with mean annual temperature.

3. Patterns of leaf thermoregulation will be a result of both plasticity and ecotypic differentiation.

Methods

To test these predictions, we measured photosynthetic heat tolerance and leaf traits in populations across a thermal gradient and predicted leaf temperatures with a leaf energy balance model. We defined leaf thermoregulation as intraspecific trait variation that led to a change in modelled [?]T ([?]T_{trait}) with an increase in mean annual temperature (MAT) or MAT of origin, with limited homeothermy present if the slope of [?]T_{trait} vs MAT is negative. We also examined genome-wide single nucleotide polymorphisms (SNP) and ran GEA and GPA analyses to explore genome-wide signals of selection and identified the environmental drivers of adaptive variation in thermoregulation using generalized dissimilarity modelling. Finally, we validated this approach in one species using a climate-controlled genotype-environment trial in a common garden glasshouse experiment.

Study system: Rainforest tree species in the Wet Tropics of Queensland, Australia

The Wet Tropics of Queensland World Heritage Area comprises 8,940 km2 of mostly rainforest vegetation in northeastern Queensland, Australia. Its mountainous terrain creates geographic and spatial variation in climatic conditions across elevation within small distances that is ideal for exploring patterns of intraspecific trait variation and local adaptation. The Wet Tropics of Queensland experiences warm temperatures year-round, with high but seasonal rainfall and periodic cyclone disturbance (UNESCO World Heritage Centre 1988). We selected three tropical rainforest species - Elaeocarpus grandis F.Muell. (Elaeocarpaceae), Cardwellia sublimis F.Muell. (Proteaceae) and Darlingia darlingiana F.Muell. L.A.S.Johnson (Proteaceae) - that are relatively abundant, upper canopy species occurring across a wide elevational range (0-1300m). Both C. sublimis and D. darlingiana are endemic to the Wet Tropics of Queensland, and have wind dispersed seeds, whereas E. grandis has a wider distribution extending into Southeast Asia and the Australian subtropics and has large fleshy fruits dispersed primarily by birds.

Field sampling

During October 2021 to May 2022, we sampled trees from 16 mature remnant forest sites from across the Wet Tropics of Queensland, spanning an elevation range of 1299 m a.s.l (5 to 1304 m a.s.l), a mean annual temperature range of 7.1degC (18.6 to 25.8degC) and a mean annual precipitation range of 2940 mm (1355 to 4295 mm). At each site 3-10 individuals per population (median 6), spaced >100 m apart to avoid sampling closely related individuals (e.g. half- or full- siblings) were selected. Sun-exposed branches from the upper canopy were sampled using a pole pruner or big shot, placed in large opaque, water-sprayed bags, and kept shaded during transport to the field lab (up to 4 hours). At the lab, branches were recut underwater in buckets and rehydrated in the dark for trait measurements (*c.* 3 hours for functional traits and 12 hours for chlorophyll fluorescence). Leaf samples for genomic analysis were dried on silica. In total we measured leaf traits on 105 *C. sublimis* , 96 *D. darlingiana,* and 104*E. grandis* individuals, and generated genomic data for 98*C. sublimis* , 96 *D. darlingiana* and 89 *E. grandis* individuals (Table 1). Additionally, seeds were collected from 11*E. grandis* individuals from six sites for the glasshouse experiment (Figure 1, Table 1).

Leaf traits

We measured leaf traits known to reflect trade-offs between resource acquisition and conservation strategies (Wright et al., 2004) as well as those impacting leaf energy balance. These included leaf mass per area (LMA, g m^{-2}), leaf dry matter content (LDMC, mg g^{-1}), leaf thickness (μm), leaf width (cm), leaf reflectance spectra including absorptance (Abs, %) and reflectance (Ref, %) to shortwave radiation, leaf carbon isotope

composition ($\delta^{13}C$), leaf nitrogen (%), and the mass ratio of carbon to nitrogen. We also measured stomatal density (stoma mm^{-2}) and size (μm^2), to calculate theoretical maximum conductance (g_{max}, mol $m^{-2}s^{-1}$). Leaf traits were measured according to standard techniques on fully expanded sun-exposed leaves from each tree (Perez-Harguindeguy et al., 2013), with 10 leaf replicates for leaf functional traits and 3 for absorptance and stomatal traits (for detailed measurement protocols, see Supplementary Material, Methods S1).

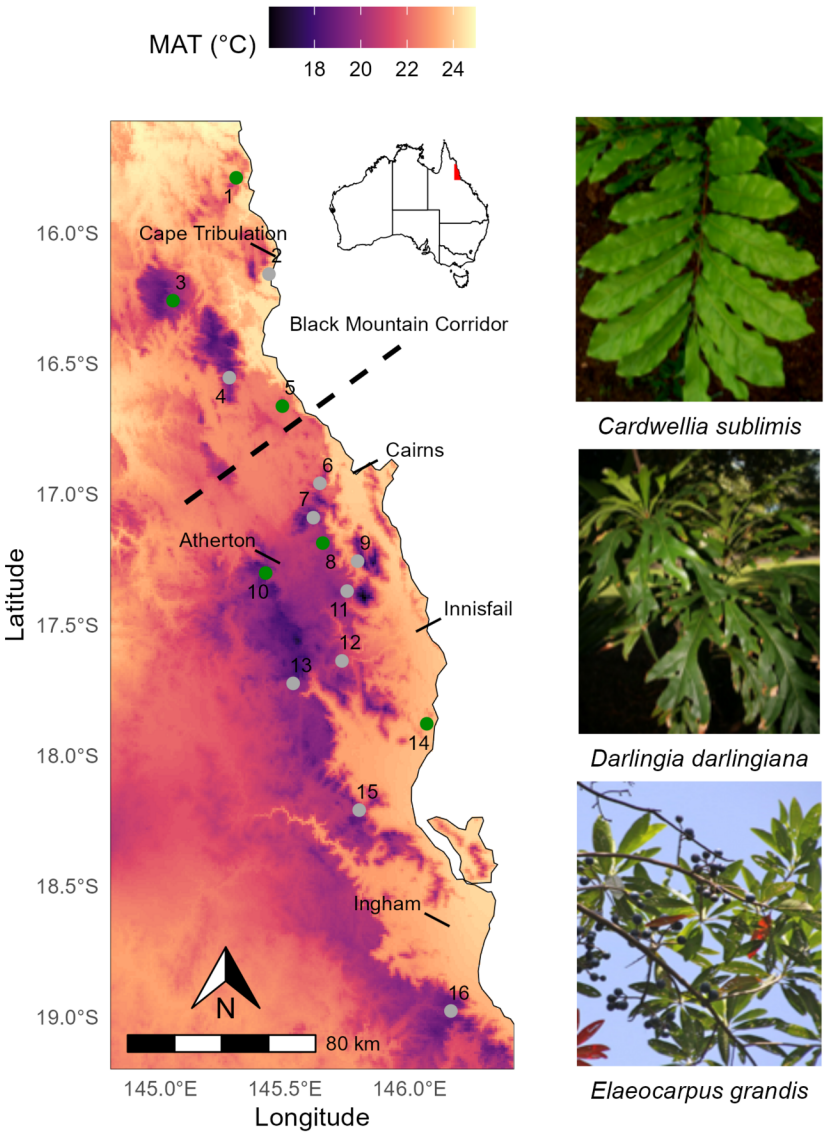

Figure 1. Map of study region. Map colour shows the mean annual temperature from 1981 to 2010 retrieved from CHELSA database at 1 km resolution (Karger et al., 2017). Dashed black line indicates position of the Black Mountain Corridor, a putative geographic barrier during glacial maxima (Schneider et al., 1998). Grey points labelled with numbers indicate the populations where genetic and trait samples were collected for each of the three species shown to the right (see Table 1 for further information on populations). Green points highlight populations where *E. grandis* seedlings were collected and used in the subsequent glasshouse

experiment.

Table 1. Site coordinates and means for environmental variables. Sites are ordered by decreasing latitude, and numbers correspond to those in Figure 1. Sample size per population is given for trait measurements, and, where this differs, for the genetic dataset in brackets.

Population	Lat.	Long.	Elev	MAT	MAP	Sample size per population		
	(°)	(°)	(m)	(°C)	(mm)	CS	DD	EG
1. Cedar Bay*	-15.79	145.3	172	23.8	2348	6	6	6
2. Daintree	-16.16	145.44	43	24.1	3296	6(5)	6	6(5)
3. Mt Windsor*	-16.26	145.05	1098	19.2	1651	6	6	6(5)
4. Mt Lewis	-16.55	145.28	1028	19.3	1790	9(8)	6	6
5. Kuranda*	-16.66	145.49	450	22.1	1957	6	6	6
6. Dinden	-16.96	145.64	493	21.7	1830	6	4	6
7. Mt Edith	-17.09	145.62	977	19.2	1907	6	6	3
8. Danbulla*	-17.19	145.65	770	20.0	2332	10(8)	9	10(6)
9. Goldsborough	-17.26	145.79	149	23.0	3072	0	6	6
10. Mt Baldy*	-17.3	145.42	1162	18.4	1555	7	6	5(4)
11. Topaz	-17.37	145.75	743	19.8	3680	6	0	6
12. South Johnstone	-17.64	145.73	540	20.6	3556	8(7)	8	8(6)
13. Tully Falls	-17.72	145.53	870	19.3	2123	6	6	6
14. Mission Beach*	-17.88	146.07	28	23.6	3545	10(7)	7	10(6)
15. Kirrama	-18.21	145.8	677	20.1	2548	6	6	6
16. Paluma Range	-18.98	146.17	832	19.2	1839	8	8	8(6)

Note: Lat = latitude, Long = longitude, Elev = elevation (m a.s.l), MAT = mean annual temperature (Bio1, °C), MAP = mean annual precipitation (Bio12, mm). CS = *Cardwellia sublimis* , DD = *Darlingia darlingiana* , and EG = *Elaeocarpus grandis* . Sites with an * had *E. grandis* seedings included in the glasshouse trial.

Leaf temperature (T_{leaf}) modelling

We tested how covariation of leaf traits affects predicted leaf-to-air temperature differences ([?]T) across a thermal gradient and whether this helps maintain T_{leaf} within safe margins. T_{leaf} was predicted using a steady-state leaf energy balance model based on the Penman-Monteith equation (Jones, 2013; Monteith & Unsworth, 2013), requiring plant trait-based inputs (leaf width, absorptance to shortwave radiation, stomatal ratio, and conductance), and microclimate inputs (air temperature, vapour pressure deficit, radiation, and wind speed).

Microclimate inputs were paramaterised using the *micro_global* function in 'NicheMapr' v.3.2.0 (Kearney & Porter, 2020) which uses the New et al. (2002) global monthly climate database at 10x10km grid centred on 1960 to 1990. Hourly estimates of T_{air}, VPD, and solar radiation (converted to photosynthetic photon flux density, PPFD) were obtained for the 15th of each month, using tree coordinates and elevation, with solar radiation adjusted for terrain using the 'microclima' setting (Maclean et al., 2019). From this typical monthly diel-data daytime means (09:00 to 15:00) were calculated for each individual tree as well as on overall mean across all individuals and species.

To separate changes in [?]T due to microclimate from those due to leaf trait covariation, we used two microclimate parameterisations when running the leaf energy balance model. For [?]T based solely on leaf traits (hereafter $[?]T_{trait}$), microclimate inputs were set to the overall daytime means described above, with T_{air}= 24.8degC, VPD = 1.4 kPa, PPFD = 1403 µmol m^2s^{-1}, and assuming calm conditions with wind speed

of 0.5 m s^{-1}. For [?]T based on both traits and climate ([?]T_{clim}), we used observed tree-level microclimate means.

We implemented the leaf energy balance model using the *PhotosynEB* function in 'plantecophys' v.1.4-6 (Duursma, 2015), which couples an energy balance model to the Farquhar, von Caemmerer and Berry photosynthesis model (Farquhar et al., 1980) and the optimality-based unified g_s (USO) model (Medlyn et al., 2011), with T_{leaf} solved iteratively. For methodological comparison we also calculated g_s from stomatal anatomy, however this was not used for downstream genetic analysis. For details on how parameters were obtained for both stomatal conductance models see Supplementary Material, Methods S1.

To convert estimated T_{leaf} to [?]T, we used the same T_{air} values used as inputs for each respective model (i.e. a common T_{air} = 24.8°C for [?]$T_{trait}$and a tree-level T_{air} for [?]T_{clim}).

Photosynthetic heat tolerance

Photosynthetic heat tolerance was assessed by examining the decline in maximum photosynthetic efficiency of photosystem II with increasing incubation temperature. To do so, the ratio of variable fluorescence (F_v) to maximum fluorescence (F_m) was measured following an established protocol (Leon-Garcia & Lasso, 2019) modified from Krause et al. (2013). For each tree, 15-20 rehydrated leaves were sampled, and six 9 mm leaf discs per leaf were pooled and randomly assigned to heat treatments. Discs were incubated for 30 minutes in water baths at 36, 40, 42, 44, 46, 48, 50, 52, 54, and 58degC, with an untreated control at ˜24degC. After a 24-hour dark incubation, chlorophyll fluorescence was measured using a PAM-2000 chlorophyll fluorometer (PAM-2000, Heinz Walz GmbH, Effeltrich, Germany). Five sites (six for *E. grandis*) at varying elevations were measured during October-November 2021. Individuals showing photoinhibition (control Fv/Fm < 0.6) were excluded from analysis. A 4-parameter log-logistic curve was fitted using 'drc' v.3.0-1 (Ritz et al., 2015), with the lower asymptote set to 0. Thermal tolerance metrics including T_{crit} (T_{leaf}at 5% decline in F_v/F_m) and T_{50} (T_{leaf} at 50% decline in F_v/F_m), were obtained from the curves.

Quantification of thermal safety margins

To determine how intraspecific trait variation influences thermal safety margins (TSM) across species distributions, TSMs were calculated by subtracting modelled T_{leaf} (=[?]T + T_{air}) from the thermal tolerance metric T_{50}. We calculated TSMs using both [?]T_{trait} and [?]T_{clim}, where [?]T_{trait} assesses the contribution of trait variation to TSMs, and [?]T_{clim} evaluates if this variation can counteract environmental changes. Our estimated TSM values likely overestimate those from direct T_{leaf}measurements, partly due to using T_{50} as the upper threshold instead of T_{crit}. Canopy leaves of tropical forests already surpass T_{crit} (Doughty et al., 2023), and while some photosynthetic function can recover after a single T_{crit} exposure, recovery is less likely after T_{50} exposure (Cook et al., 2024; Tarvainen et al., 2022). Additionally, microclimate inputs (e.g. T_{air}) used for modelling T_{leaf} are daytime averages (09:00 to 15:00). Although selection is often driven by climate extremes rather than means (Zimmermann et al., 2009), our conservative approach is suitable for modelling relative [?]T_{trait} across a species distribution.

Climate and Environmental Variables

To explore environmental drivers of trait and genomic variation, we retrieved gridded maps of bioclimatic variables, as well as wind speed and relative humidity for the Wet Tropics of Queensland from the CHELSA database at 1km resolution, averaged for 1981-2010 (Brun et al., 2022; Karger et al., 2017). Gridded soil data products at 5-15 cm depth, 30m resolution, for the period 1950–2013 were obtained from the Soil and Landscape Grid of Australia and resampled to 1 km resolution using 'raster' v.3.6-11 (Hijmans, 2022) to match the bioclimatic data. To avoid multicollinearity and ensure interpretability, we selected uncorrelated variables ($r < 0.7$, calculated using values for the sampled sites) relevant to tropical tree functioning: mean

annual temperature (Bio1,degC), precipitation of the driest month (Bio14, mm), minimum relative humidity (RH_{min}, %), mean wind speed ($Wind_{mean}$, m s^{-1}), soil pH (pH), and total soil phosphorus (P).

Genotyping

Dried leaf tissue samples were sent to Diversity Arrays Technology Australia Pty Ltd, Canberra, Australia for DNA extraction and genotyped using DArTseq, a reduced representation sequencing method (Sansaloni et al., 2010). Data quality and SNP filtering were performed using 'RRtools' v.0.1 (Bragg et al., 2020; Rossetto et al., 2019). SNPs with a reproducibility score below 0.96, over 20% missing data, or redundant loci were excluded. Individuals with 80% missing loci were also removed and a minor allele frequency threshold of 0.05 was applied. The cleaned dataset comprised 8884 SNPs across 98 individuals from 15 populations for *C. sublimis* (6.48 % missing data), 8009 SNPs across 96 individuals from 15 populations for *D. darlingiana* (8.15 % missing data), and 4935 SNPs across 89 individuals from 16 populations for *E. grandis* (6.65 % missing data).

Population genetic diversity and structure

We assessed population genetic diversity by estimating allelic richness, expected heterozygosity (He), observed heterozygosity (Ho) and the inbreeding coefficient (FIS) using 'diveRsity' v1.9.90 (Keenan et al., 2013), with 1000 bootstrap replicates for confidence intervals. Genetic similarity was evaluated through Principal Component Analysis (PCA) using 'adegenet' v2.1.8 (Jombart, 2008). Overall FST for each species was estimated from analysis of molecular variance on all SNPs using the 'poppr' package and was converted into $\chi 2$ distribution. This was compared with PST estimates and 95% confidence intervals for each trait. Ancestry coefficients were estimated via discriminant analysis of principal components (DAPC) and sparse non-negative matrix factorization (sNMF). For both methods, we tested genetic clusters (K) ranging from 1 to 16. DAPC was performed with K-means clustering on PCA-transformed genotypes, selecting the optimal K via the Bayesian information criterion and retaining 10 principal component axes using cross-validation. For sNMF, 'LEA' v.3.8.0 (Frichot & François, 2015) was used, selecting the optimal K based on the stabilization of cross-entropy values and choosing the best replicate with the lowest cross-entropy.

Signals of selection

To detect potentially adaptive loci, we used F_{ST} outlier analysis, genotype-environment associations (GEA), and genotype-phenotype associations (GPA). Association analyses were performed using latent factor mixed modelling (LFMM) and partial redundancy analysis (pRDA). This approach combined univariate and multivariate methods to detect both single-locus and multi-locus signatures of selection with high power and low false-positive rates (Forester et al., 2018). For GPA, we tested two trait sets: 1) [?]T_{trait} as an integrative trait, and 2) a suite of uncorrelated ($r < 0.7$) leaf traits influencing leaf temperature including LMA, thickness, width, Absorptance, V_{cmax}, and g_1.

To ensure complete SNP datasets, missing values were imputed with the most common allele across individuals. Given the multiple potential values of K identified in prior population structure analyses, we conducted analyses for K = 1, 2, and 3, treating all significant SNPs as putatively adaptive. F_{ST} outlier analysis was done using 'pcadapt' v.4.3.3 (Luu et al., 2017) using default parameters, with SNPs considered putatively adaptive if the qvalue was < 0.05. LFMM was run for both GPA and GEA analyses with a lasso penalty using 'lfmm' v.1.1 (Caye et al., 2019) testing multiple latent factors. Z scores were calibrated for genomic inflation before being converted into p-values. Candidate SNPs were identified using a false discovery threshold of $q < 0.1$. The pRDA analyses in both GPA and GEA were conducted using 'vegan' v.2.6-4 (Oksanen et al., 2022), with two principal components for genetic structure (see previous section) as conditional variables. For GPA, elevation was also included as a conditional variable to account for non-genetic variation in leaf traits. SNPs associated with phenotypes (GPA), or environments (GEA) were identified by extreme loadings, defined as 3 standard deviations along pRDA axes.

Generalised dissimilarity modelling

We employed generalised dissimilarity modelling (GDM) to further investigate non-linear genotype-environment and phenotype-environment associations and identify potential environmental drivers of variation. In contrast to LFMM and pRDA, this approach assesses multivariate, nonlinear patterns of genomic or trait turnover along environmental gradients, while accounting for isolation by distance (Ferrier et al., 2007; Mokany et al., 2022). GDM is useful for evaluating the relative importance of environmental predictors (via the sum of I-spline coefficients) and for identifying where steepest gradients of change occur (by observing the change in slope).

For the genomic data, we ran GDMs on three SNP datasets. First, we used the putatively adaptive SNPs identified through trait associations (GPA analysis), including all those identified by LFMM and pRDA with leaf traits or estimated [?]Ttrait. The second dataset included SNPs identified as genomic outliers (FST outlier analysis) and through association with environment (GEA analysis). We explored both GEA and GPA datasets because GPA was not measured in a common garden; thus, GEA helps determine if the environmental variables linked to trait variation also drive adaptive variation. While the environmental drivers of genomic variation are already inherently assessed within the LFMM and pRDA analyses in GEA, we performed GDM on this SNP set to allow direct comparison of driver relative importance across the different genomic GDMs. The third dataset investigated whole genome variation across environmental space, using the original cleaned SNP set that includes both adaptive and neutral SNPs. For all three analyses, we used a population-level pairwise FST distance matrix generated with 'SNPRelate' v.1.30.1 (Zheng et al., 2012) using the relative beta estimator in Weir & Hill (2002).

Additionally, we conducted two trait GDMs to assess environmental drivers of [?]Ttrait and leaf trait variation. We calculated population-level means for [?]Ttrait and other leaf traits (uncorrelated suite described above). For the leaf trait GDM, we reduced variables to two principal component axes using the princomp function. Euclidean distance matrices were computed for each dataset using the dist function. All five GDMs were fit using 'gdm' v.1.5.9-9.1 (Ferrier et al., 2007; Mokany et al., 2022). Predictor significance was tested with matrix permutation (n = 50 permutations) using the gdm.varImp function, with predictor significance defined by increases in explained deviance. Variables with the highest sum of I-Spline Coefficients were considered most important. We estimated model sensitivity with bootstrapping (n = 1,000 iterations), retaining 90% of populations (Shryock et al., 2015).

Glasshouse experiment

We collected 59 naturally germinated *E. grandis* seedlings from the base of 11 likely mother trees across six sites and grew these in pots at James Cook University's Environmental Research Complex in Cairns (Figure 1). The number of mother trees per site ranged from one to three, and seedlings per mother tree ranged from one to two. Seedlings originated from sites with mean annual temperatures between 18.8degC and 24.9degC.

To assess genotype x environment effects on leaf thermal traits while controlling for temperature and vapor pressure deficit (VPD) variations, we conducted a glasshouse experiment with three treatments: a cool-humid chamber (26degC, 1 kPa VPD), a warm-humid chamber (32degC, 1 kPa VPD), and a warm-dry chamber (32degC, 2 kPa VPD). These treatments simulated typical upland summer conditions (cool-humid) and lowland conditions (warm-dry), with the warm-humid chamber used to isolate VPD effects from temperature effects (Table S 1).

In August 2022, seedlings were allocated to their respective chambers, with at least one seedling from each mother tree in each chamber. After two months, leaf-level gas exchange and functional traits were measured on new, fully expanded sun leaves. Two seedlings in the cool-humid treatment died, leaving 57 seedlings but maintaining the total number of mother trees in that treatment. Detailed measurement protocols are described in Supplementary Material, Methods S2.

Our goal was to assess how genotype and environment contribute to intraspecific variation in leaf thermoregulation and to determine if plants acclimated or adapted to warmer conditions have lower predicted [?]T_{trait} compared to those acclimated or adapted to cooler conditions.

We first quantified intraspecific variation, population differentiation, and the association of trait variation with thermal gradients. This involved using the quartile coefficient of variation to account for issues with standard CV (Botta-Dukat, 2023). Linear regressions assessed the relationship between leaf functional traits (e.g., LMA, LDMC, leaf thickness, $\delta^{13}C$) and thermal parameters (e.g., T_{crit}, T_{50}, [?]T_{trait}, TSM) with population identity or mean annual temperature (MAT) as dependent variables. Population differentiation was measured using R^2, which is analogous to P_{ST} but does not assume trait heritability. A negative slope in [?]T_{trait} with increasing MAT was interpreted as evidence of limited homeothermy.

To examine if trait variation was an adaptation to temperature across species distributions, we identified signals of selection using association analysis and compared the relative importance of environmental predictors in genomic vs trait generalized dissimilarity modelling. To complement association analyses and explicitly test the contribution of genotype and environment to intraspecific variation in leaf traits and [?]T_{trait} for *E. grandis* saplings grown in a glasshouse, we used mixed effects models to test the influence of MAT of origin (continuous) and treatment (cool-humid, warm-humid, warm-dry) on leaf traits and [?]T_{trait}, including 'mother tree' as a random effect nested within 'site'. We then removed non-significant variables and presented estimated marginal means for the final models.

Results

Extent of intraspecific leaf trait variation in natural populations

In most cases, the extent of intraspecific trait variation (defined as the quartile coefficient of variation, CV) for each trait was similar across the three species (Figure 2a). Traits with the lowest quartile CV (< 0.05) included LDMC, Absorptance, Reflectance, $\delta^{13}C$, T_{crit}, and T_{50}. The trait g_{1}, which is calculated from $\delta^{13}C$ (but accounts for some influence of the environment) had the highest levels of variation and showed the greatest differences in CV across species, with CV = 0.14, 0.28, and 0.21 in *C. sublimis* , *D. darlingiana* , and *E. grandis* respectively. For most traits, population effects on trait variation were significant ($P < 0.05$), except for leaf C/N ratio, $\delta^{13}C$, g_{1}, and T_{50} in *C. sublimis* ; stomatal density, T_{crit} and T_{50} in *D. darlingiana* ; and stomatal density, theoretical g_{max}, and T_{crit} in *E. grandis* (Figure 2a, Table S2). Where significant effects of population on trait variation were observed, the proportion of trait variation explained by population ranged from 23% to 85% across all species and traits, with the strongest effects observed for leaf thickness (Figure 2a, Table S2). Population differentiation for most traits was stronger than expected due to genetic drift ($P_{ST} > F_{ST}$), except for leaf elemental concentrations or thermal tolerance metrics in *C. sublimis* (Figure S1).

Patterns of leaf trait variation with mean annual temperature

We observed differences in the relationship between traits and mean annual temperature (MAT) across the three target species (Figures 2b & S2, Table S3). In *C. sublimis* , g_{1} was the only trait associated with MAT despite other traits having levels of CV similar to the other species and significant population effects on trait variation (Figures 2b & S2, Table S3). For *D. darlingiana* , as MAT increased, LMA, leaf thickness, Absorptance, and $\delta^{13}C$ all decreased, whereas leaf width andg_{1} increased (Figure 2b, Figure S2, Table S3). However, the effect of MAT on leaf thickness, absorptance, and anatomical thermal safety margin was weak ($R^2 < 0.1$). In*E. grandis* , as MAT increased, LMA, leaf width, $\delta^{13}C$, and stomatal size decreased, whereas LDMC,g_{1} and stomatal density increased (Figure 2b, Figure S2, Table S3), but this association was weak for LMA, LDMC, and $\delta^{13}C$. For *D. darlingiana* and *E. grandis* , the covariation between stomatal density and size resulted in no change in theoretical g_{max} with MAT (Figure 2b, Figure S2, Table S3).

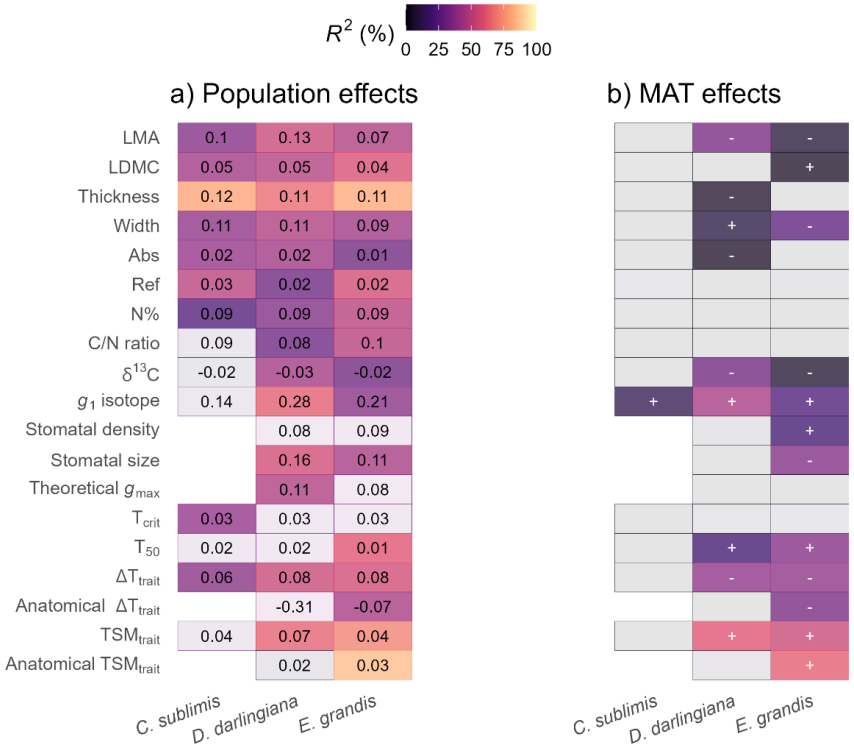

Figure 2. Comparison of regression results for the effect of population or mean annual temperature on trait variation for each species. Tiles are coloured by R^2, with transparent tiles indicating non-significant ($P > 0.05$) results. Values within tiles for panel a) show the quartile coefficient of variation, and symbols in panel b) show the sign of the slope estimate for the linear regression. For more information on model results see Table S 2 and Table S 3.

Implications of intraspecific trait variation on leaf thermoregulation and thermal safety margins

The consequences of intraspecific trait trade-offs for leaf thermoregulation were investigated through the prediction of trait-based leaf-to-air temperature differences ($[?]T_{trait}$) and how these vary with MAT. Note that $[?]T_{trait}$ is calculated using a single set of microclimate parameters and thus represents the influence of traits only. Mean $[?]T_{trait}$ was 6.0, 5.1, and 4.2°C in *C. sublimis* , *D. darlingiana* , and *E. grandis* respectively (Table S2). Levels of intraspecific variation in $[?]T_{trait}$ were similar across the three species, with quartile CV = 0.06 to 0.08 (Figure 2a). Population was a significant predictor of $[?]T_{trait}$ for all species, although the proportion explained was slightly higher for *D. darlingiana* and*E. grandis* than *C. sublimis* (Figure 2a, Table S2). We found evidence of leaf thermoregulation for two of the three species, with $[?]T_{trait}$ decreasing with increasing MAT for *D. darlingiana* ($R^2 = 0.39$, $P < 0.001$) and *E. grandis* ($R^2 = 0.39$,$P < 0.001$) but not *C. sublimis* (Figure 2b, Figure 3, Table S3). This represented a 0.21degC (95^{th}C.I. 0.15, 0.26) and a 0.16degC (95^{th} C.I. 0.12, 0.20) decrease in $[?]T_{trait}$ per 1degC increase in MAT for *D. darlingiana* and *E. grandis* respectively (Table S3).

Unsurprisingly, using theoretical g_{max} from stomatal anatomy to calculate trait-based leaf-to-air temperature differences (anatomical $[?]T_{trait}$) led to substantially lower values of $[?]T_{trait}$ (Figure S3). Mean anatomical $[?]T_{trait}$ was equal to -0.6degC for *D. darlingiana* and -1.8degC for *E. grandis* (with negative values indicating T_{leaf} cooler than T_{air}). Levels of intraspecific variation for anatomical $[?]T_{trait}$ in*D. darlingiana* and *E.*

grandis were different, with a quartile CV = -0.31 for *D. darlingiana* and -0.07 for *E. grandis* (Figure 2a). Population was only a significant predictor of anatomical [?]T_{trait} for *E. grandis* , with$R^2 = 0.45$, $P = 0.014$ (Figure 2a, Table S2). This time we found evidence of thermoregulation only for *E. grandis* ($R^2 = 0.33$, $P < 0.001$) where anatomical [?]T_{trait} decreased 0.06degC (95^{th} C.I. 0.03, 0.09) per 1degC increase in MAT (Figures 2b & S3, Table S3).

Thermal tolerance metrics were similar for all three species, with species-mean T_{crit} ranging from 44.3 to 45.1degC and species-mean T_{50} ranging from 49.5, to 49.8degC (Table S2). Levels of intraspecific variation were low relative to other traits, and population differences were only significant in *C. sublimis* for T_{crit} and *E. grandis* for T_{50} (Figure 2a, Table S2). We observed significant positive relationships between T_{50} and MAT for both*D. darlingiana* and *E. grandis* , but not *C. sublimis* , and no relationship between MAT and T_{crit} for any species (Figures 2b & 3, Table S3). T_{50} increased by 0.22degC per 1degC rise in MAT for *D. darlingiana* ($R^2 = 0.19$, $P = 0.044$), and 0.28 degC per 1degC rise in MAT for *E. grandis* ($R^2 = 0.28$, $P < 0.001$, Figure 3).

The combined variation in T_{50} and [?]T_{trait} were assessed through calculation of trait-based thermal safety margins (TSM_{trait} = T_{50} - T_{leaf} degC). We observed a significant increase in TSM_{trait} with MAT for *D. darlingiana* and *E. grandis* , but not *C. sublimis* , representing an increase in TSM_{trait} of 0.52degC (95^{th} C.I. 0.32, 0.72) and 0.42degC (95^{th} C.I. 0.26, 0.58) per 1degC increase in MAT for *D. darlingiana* and *E. grandis* respectively (Figures 2b & 3, Table S3). In contrast, when calculating trait-based thermal safety margins using stomatal anatomical traits (anatomical TSM_{trait}), we only observed a relationship with MAT in *E. grandis* ($R^2 = 0.62$,$P < 0.0001$), representing an increase in TSM_{trait} of 0.4degC (95^{th} C.I. 0.22, 0.58 per 1degC increase in MAT (Figures 2b & S3, Table S3).

To evaluate how effective intraspecific trait variation was at avoiding heat stress in-situ, we compare the above results with [?]T (and TSMs) calculated using tree-level variation in both traits and microclimate ([?]T_{clim} and TSM_{clim}) (Figure 3). A comparison of slope estimates for the linear regression of [?]T_{trait} and [?]T_{clim} with MAT indicated that our approach of excluding the passive effects of site microclimate in [?]T_{trait} leads to a 0.08 and 0.09degC shallower decrease in [?]T_{trait} with MAT compared to [?]$T_{clim}$for *D. darlingiana* and *E. grandis* respectively, and no change for *C. sublimis* (Figure 3, Table S3). Comparing slopes for the linear regression of TSM_{clim} with MAT across species that exhibited [?]T_{trait} variation consistent with limited homeothermy (*D. darlingiana* and *E. grandis*) with that which did not (*C. sublimis*) highlights how effective thermoregulation could be at offsetting increasing air temperatures in TSM_{clim}. We found that the TSM_{clim}decline with MAT was significantly shallower for *D. darlingiana* (Slope = -0.55, $R^2 = 0.59$, $P < 0.001$) and *E. grandis* (Slope = -0.63, $R^2 = 0.66$, $P < 0.001$) compared to *C. sublimis* (Slope = -1.11, $R^2 = 0.85$, $P < 0.001$) (Figure 3, Table S3).

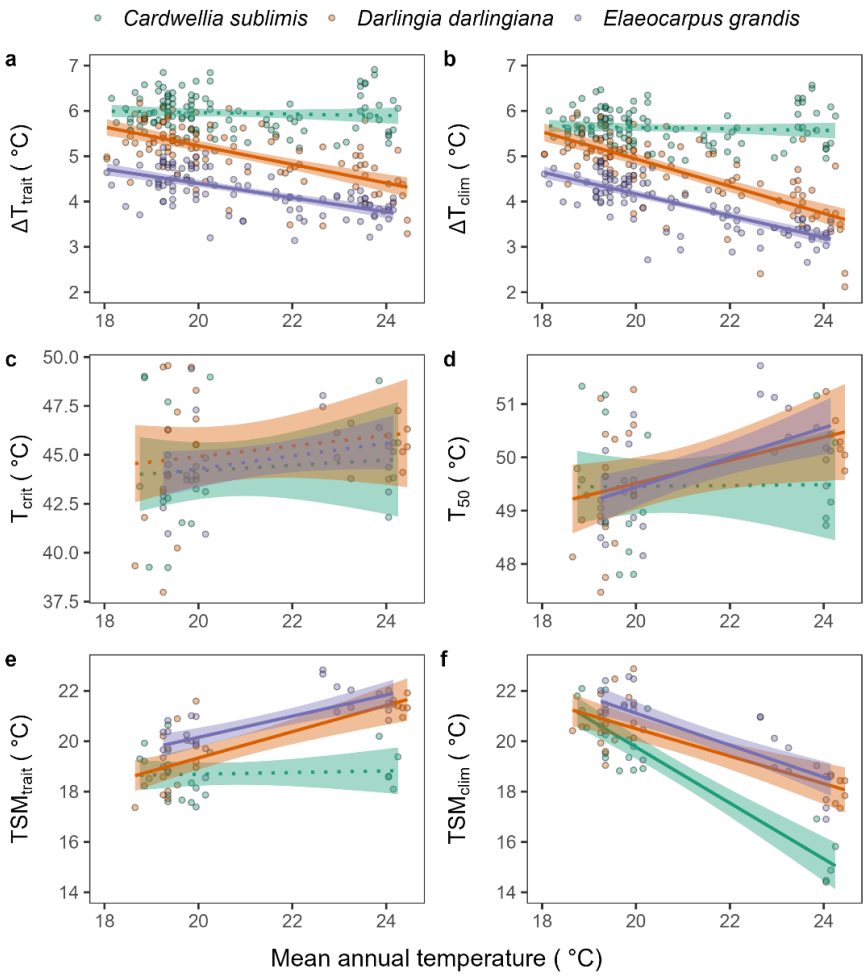

Figure 3. Variation in leaf-to-air temperature differences ([?]T; a-b), thermal tolerance metrics (T_{crit} & T_{50}; c, d) and thermal safety margins (TSM; e, f) with mean annual temperature across the distribution of three tropical tree species. Note in a, b, and e [?]T is based on leaf trait variation with the same microclimate inputs for all trees ([?]T_{trait}), whereas in f, microclimate inputs also vary with each individual tree ([?]T_{clim}). Each point represents an individual-tree level average. Significant correlations with mean annual temperature are denoted by solid regression lines whereas non-significant correlations are dotted. Shaded region represents standard errors.

Genetic diversity and population structure

Genetic diversity was relatively low in our study species. Expected heterozygosity across all populations was 0.19 (±0.012 SD) in *C. sublimis* , 0.19 (±0.011 SD) in *D. darlingiana* , and 0.23 (±0.013 SD) in *E. grandis* (Table S 4). Observed heterozygosity was less than expected heterozygosity for all populations of all species and was 0.15 (±0.014 SD) in *C. sublimis* , 0.12 (±0.010 SD) in *D. darlingiana* , and 0.18 (±0.016 SD) in *E. grandis* (Table S 4). All three species showed strong isolation by distance, with mantel tests showing R^2 of 0.86 ($P = 0.001$) in *C. sublimis* (Figure S 4), R^2 of 0.77 ($P = 0.001$) in *D. darlingiana* (Figure S 5), and R^2 of 0.51 ($P = 0.011$) in *E. grandis* (Figure S 6). Ancestry analysis indicated the presence of 1, 2, or 3 genetic clusters across the sampled range, supported by PCA analysis, with the main break for all species corresponding to the Black Mountain Corridor, a biogeographic barrier for multiple taxa coinciding with a

break in the Great Dividing Range (Figures S4-6) (Schneider et al., 1998).

Signals of Selection

We identified signals of selection in all three species through the detection of candidate SNPs that were associated with either environmental (GEA) or phenotypic (GPA) variables or were identified F_{ST} outliers.

For *C. sublimis* , the genotype-phenotype association (GPA) analyses identified 118 candidate SNPs associated with [?]T_{trait} or leaf traits themselves (Figure 4, Table S5). LFMM identified 1 SNP associated with leaf thickness and no SNPS associated with predicted [?]T_{trait}. The leaf trait pRDA had an adjR^2 = 0.0031 and identified 66 SNPs with the highest contributing variables including leaf thickness, LMA, Absorptance, and V_{cmax25} (Figure S7a). The [?]T_{trait} pRDA had an adjR^2 of 0.0006 and identified 63 candidate SNPs. The combined F_{ST}outlier and GEA analyses identified 321 unique candidate SNPs, including 243 SNPs identified by F_{ST} outlier analysis and 85 SNPs identified by GEA (Figure 4, Table S5). For the GEA SNPs, LFMM identified 13 SNPs including 1 associated with Bio1, 4 with RH_{min}, 3 with $Wind_{mean}$, 1 with Bio14, 2 with Soil P and 2 with Soil pH. The environment pRDA had an adjR^2 = 0.0173 and identified 72 candidate SNPs, with highest contributing variables including Bio1, Bio14, RH_{min} and $Wind_{mean}$ (Figure S7b). In*C. sublimis* , 1 candidate SNP was identified by GPA, GEA, and outlier analyses, 4 candidate SNPs were identified both by GPA and GEA analyses, and 4 SNPs were identified by both GPA and outlier analyses (Figure 4).

For *D. darlingiana* , the GPA analyses identified 151 candidate SNPs associated with [?]T_{trait} or leaf traits themselves (Figure 4, Table S5). LFMM identified 43 SNPs associated with one or more leaf traits including 2 SNPs associated with leaf width, 11 withg_{1}, 25 with V_{cmax25}, 2 with LMA and 3 with modeled [?]T_{trait}. The trait pRDA had an adjR^2 = 0.0022 and identified 63 SNPs with the highest contributing variable being Absorptance, g_{1}, and LMA (Figure S7c). The [?]T_{trait} pRDA had an adjR^2 of 0.0006 and identified 69 candidate SNPs. The combined F_{ST} outlier and GEA analyses identified a total of 140 unique candidate SNPs, including 60 SNPs identified by F_{ST} outlier analysis and 87 SNPs identified by GEA (Figure 4, Table S5). For the GEA SNPs, LFMM identified 24 SNPs, including 3 SNPs associated with Bio1, 3 with RH_{min}, 1 with $Wind_{mean}$, 3 with Bio14, 13 with Soil P, and 2 with Soil pH. The environment pRDA had an adjR^2 = 0.0083 and identified 63 candidate SNPs, with highest contributing variables including MAT and soil pH, followed by Bio14, RH_{min}, and $Wind_{mean}$ (Figure S 7d). In *D. darlingiana* , 2 candidate SNPs were identified both by GPA and GEA analyses, and 1 SNP was identified by both GPA and outlier analyses (Figure 4).

For *E. grandis* , the GPA analyses identified 73 candidate SNPs associated with [?]T_{trait} or leaf traits themselves (Figure 4, Table S5). LFMM identified 4 SNPs including 1 SNP associated with leaf width, 2 with LMA, and 1 with [?]T_{trait}. The trait pRDA, had an adjR^2 = 0.0019 and identified 28 candidate SNPs, with the highest contributing variables includingV_{cmax25}, leaf thickness, and LMA, followed by Absorptance and leaf width (Figure S7e). The [?]T_{trait}pRDA had an adjR^2 of 0.0006 and identified 45 candidate SNPs. The combined F_{ST} outlier and GEA analyses identified 156 unique candidate SNPs, including 126 SNPs identified by F_{ST} outlier analysis and 30 SNPs identified by GEA (Figure 4, Table S5). For the GEA SNPs, LFMM identified 1 SNP associated with Bio1. The environment pRDA had an adjR^2 of 0.0064 and identified 29 SNPs, with the highest contributing environmental variables including Bio14, RH_{min}, soil P, and MAT (Figure S7f). In *E. grandis* , no candidate SNPs were identified both by GPA and GEA analyses, however 1 SNP was identified by both GPA and outlier analyses (Figure 4, Table S5).

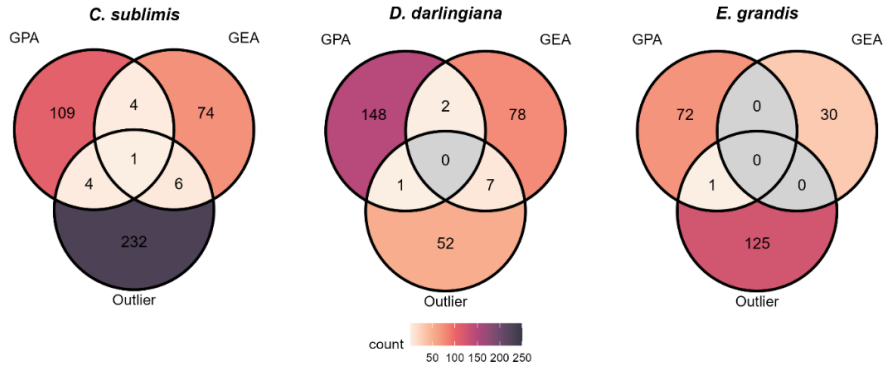

Figure 4. Overlap of candidate SNPs identified using F_{ST}outlier analysis, and genotype phenotype (GPA) and genotype environment (GEA) association analyses for three tropical tree species. Numbers indicate the total number of overlapping SNPs with each analysis. Candidate SNPs identified using GPA or GEA association analyses include all identified by either latent factor mixed modelling (LFMM) or partial redundancy analysis (pRDA). For GPA analyses, candidate SNPs include those identified from two sets of response variables; '[?]T_{trait}', based on modelled leaf-to-air temperature differences with individual tree level traits and common microclimate inputs, and 'Trait PCA', based on the principal component axes of a suite of leaf traits. Intersections are coloured by total number of SNPs and with grey panels = no shared SNPs detected.

Generalised dissimilarity modelling

We used generalized dissimilarity modelling to investigate the relative importance of environmental predictors in explaining deviance in the genotypic turnover across the landscape based on GPA SNPs, GEA and outlier SNPs, and all SNPs, as well as trait turnover in [?]T_{trait}, and in the principal components of leaf functional traits as the response matrices. Across all three species, the GDMs based on SNP datasets had generally high explained deviance (27.47–76.89%) and low intercepts (0–0.07), indicating the included predictors had good explanatory power. In contrast, the GDMs based on [?]T_{trait} or the leaf trait PCA values explained less variance in the response variables (explained deviance 20.93–44.07%, intercepts 0.07–0.44) (Table S6).

In *C. sublimis* , geographic distance was the top predictor of allele frequency turnover for all three SNP-based GDMs, followed by soil pH and precipitation of the driest month (Bio14) for the GPA-SNPs, Bio14 and RH_{min} for the GEA and outlier SNPs, and Bio14 and $Wind_{mean}$ for the All SNPs GDMs (Figure 5, Table S6). For the trait GDMs, Soil pH was the most important predictor of [?]T_{trait} variation, whereas Bio14, followed by soil P were the most important predictors of variation in the Trait PCA (Figure 5, Table S6).

For *D. darlingiana* , Geographic distance, followed by MAT and Bio14 were the top environmental predictors for all three SNP-based GDMs (Figure 5, Table S6). For the trait GDMs, variation in [?]T_{trait} was best explained by MAT, whereas both MAT and Bio14 were importance predictors in the Trait PCA GDM (Figure 5, Table S6).

In *E. grandis* , geographic distance and Bio14 were the top two predictors for all SNP-based GDMs, with the third most explanatory variable switching between MAT and RH_{min} (Figure 5). In the trait GDMs, MAT was the single most important predictor for variation in both [?]T_{trait} and the trait PCA (Figure 5, Table S6).

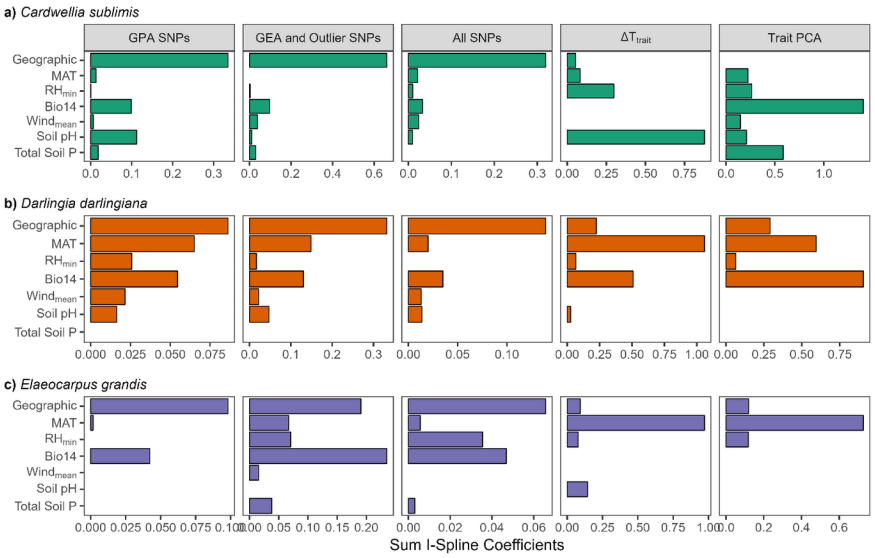

Figure 5. Relative importance of predictors in generalised dissimilarity models (GDM) for three tropical tree species. Relative importance is calculated as the sum of I-Spline coefficients for that predictor in the model. For each species there are five separate analyses presented, with the response variable a population-level pairwise FST matrix on SNPs identified by GPA analyses (GPA SNPs), the SNPs identified from GEA or FST outlier analyses (GEA and Outlier SNPs), or the entire suite of neutral and non-neutral SNPs (All SNPs). For the last two columns, the response variable was a Euclidean distance matrix based on either population-mean [?]Ttrait or principal component axes on a suite of leaf traits (Trait PCA). Model performance metrics can be found in Table S 6. For the predictor variables, Geographic = geographic distance, MAT = mean annual temperature, RHmin = minimum relative humidity, Bio14 = precipitation of the driest month, Windmean = mean wind speed.

Elaeocarpus grandis – Genotype × Environment glasshouse trial thermoregulatory traits

In the climate-controlled glasshouse experiment, E. grandis showed trait variation resulting from both plastic responses to treatment conditions, and adaptation to mean annual temperature of origin, but not their interaction (Figure 6, Table S7). Leaf width had a negative correlation with MAT of origin and had significant effects of treatment, exhibiting narrower leaves when grown under warmer conditions. We observed a significant positive correlation between g 1 and MAT of origin, but no effect of treatment. Variation in Vcmax25 was not associated with MAT of origin, but was influenced by treatment, with plants grown under cool-humid conditions having a higher Vcmax25 than plants grown under both warm-humid and warm-dry conditions (Figure 6, Table S7). When these traits were input into a leaf energy balance model paramaterised with standard microclimate to determine [?]Ttrait we found evidence for adaptation to MAT of origin but no effect of treatment (Figure 6, Table S7). Seedlings from warm-origin provenances had lower [?]Ttrait than seedlings from cool-origin provenances (Figure 6, Table S7). These patterns were driven by intraspecific variation in both leaf width and g 1. The decline in [?]Ttrait with an increase in MAT of origin is likely due to the combined effects of narrower leaves, and a higher g 1 (so lower water use efficiency), which both result in cooler Tleaf under common conditions and thus a decrease [?]Ttrait. The lack of a treatment effect on [?]Ttrait is likely due to the treatment effects on Vcmax25 and leaf width cancelling each other out. i.e. for leaves with common g 1, a higher Vcmax25 will result in a higher modelled conductance which will cool leaves.

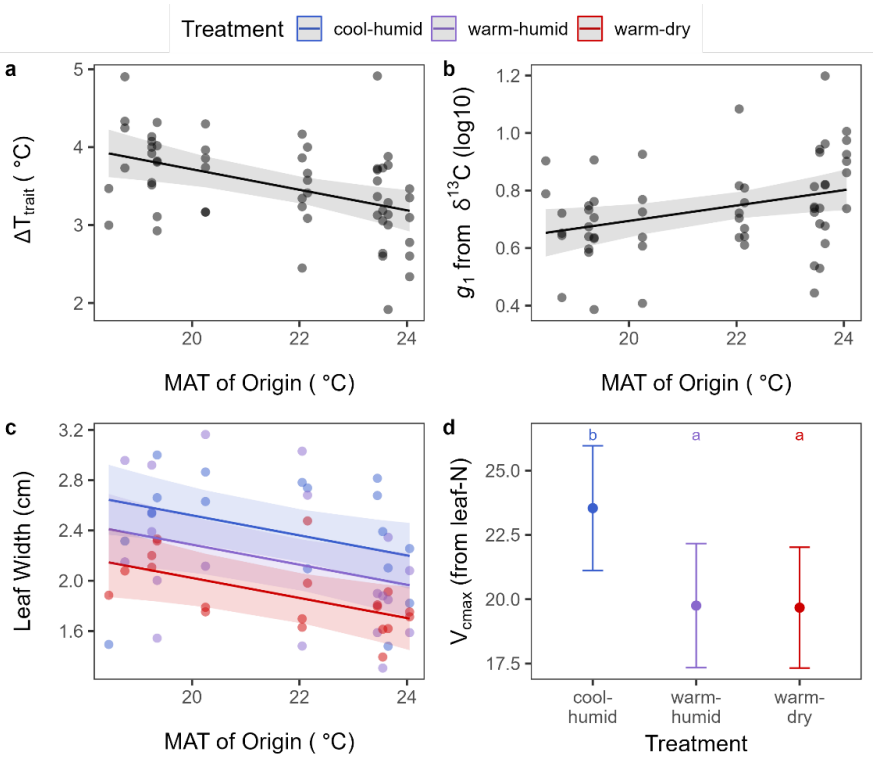

Figure 6. Results from the glasshouse experiment showing significant effects of both treatment conditions and mean annual temperature of origin in *E. grandis* . Panels show a) response of predicted leaf-to-air temperature differences based on leaf traits ([?]T_{trait}), b) g_1 calculated from leaf $\delta^{13}C$ plotted as log10 transformed values, c) leaf width, and d) V_{cmax25} estimated from leaf N_{mass}. Points represent observed plant level averages, and lines and shaded regions show the estimated margin means and 95% confidence intervals. Letters in panel d) show significant differences.

Discussion

Globally increasing temperatures threaten to push tropical rainforest plants beyond their physiological limits. However, populations adapted to contrasting climates may exhibit phenotypic divergence due to local adaptation that affects their capacity to cope with warming. Intraspecific variation of leaf traits across species distributions can enhance leaf cooling, thereby avoiding lethal temperatures in warmer regions. Yet, evidence of this thermoregulatory ability and the roles of acclimation or adaptation remain limited despite it being key information to assess population resilience to global warming impacts. Here we show how leaf energy balance modelling combined with population/ecological genomics can be used to assess the patterns and drivers of local adaptation of thermoregulatory traits in mature tropical rainforest trees. We found intraspecific variation of field-measured leaf traits was associated with enhanced leaf cooling and partial maintenance of modelled thermal safety margins in warmer sites for two of the three species, providing partial support for our first hypothesis. Signals of selection were detected in all species, however contrary to our second hypothesis, adaptive genomic variation associated with predicted [?]T_{trait} was best explained by geographic distance and precipitation of the driest month rather than temperature. Finally, our genotype $\times$ environment trial of *E. grandis* seedlings supported our third hypothesis: clines in [?]T_{trait} with MAT of origin were a result of both phenotypic plasticity and adaptation.

Intraspecific trait variation leads to enhanced leaf cooling in warmer climates.

Our expectation that leaf trait variation would enhance leaf cooling in plants from warmer sites was observed in two of the three species. This is consistent with the limited homeothermy hypothesis (Mahan & Upchurch, 1988; Michaletz et al., 2015) which suggests that trait-based regulation of leaf temperatures may help maintain carbon uptake in suboptimal environments. Although evidence for this phenomenon varies across biomes and species (Blonder et al., 2020; Drake et al., 2020; Fauset et al., 2018; Guo et al., 2023; Guo et al., 2022; Helliker & Richter, 2008; Helliker et al., 2018; Liancourt et al., 2020; Song et al., 2011; Still et al., 2022; Zhou et al., 2023), the theory is debated due to inconsistencies in its definition and testing (Still et al., 2023). By using a leaf energy balance model parameterized with observed leaf trait variations and common microclimate inputs, we isolate [?]T variations resulting from leaf trait covariation, excluding passive changes due to radiation, humidity, wind speed, and air temperature. This approach avoids the flawed assumption that limited homeothermy requires Tleaf to decrease below Tair.

We found that traits varied significantly with MAT in E. grandis and D. darlingiana, but their responses differed: leaf width increased with MAT for D. darlingiana and decreased for E. grandis . Wider leaves have lower boundary layer conductance leading to higher leaf temperatures (Leigh et al., 2017; Wright et al., 2017). Despite this, both species showed similar declines in [?]Ttrait with increasing MAT. This suggests that variables associated with stomatal conductance (g s) played crucial roles in offsetting the heating effect of wider leaves in D. darlingiana . When comparing predicted [?]Ttrait using the coupled photosynthesis-stomatal conductance model with predictions based on theoretical maximum conductance (which itself did not change with MAT), the [?]Ttrait trends aligned for E. grandis but not for D. darlingiana . Differences between the methods may partly explain the lack of thermoregulation observed by Kullberg et al. (2023) who used stomatal anatomical traits to calculate g s. The primary model we used assumes g s is coupled with photosynthesis (Medlyn et al., 2011), but this may not be true under high temperatures (De Kauwe et al., 2019; Diao et al., 2024; Drake et al., 2018; Marchin et al., 2023; Urban et al., 2017), particularly in high humidity conditions typical of tropical rainforests. Given the impact of g s modelling on our results, it is crucial to develop approaches that accurately account for how g s varies with temperature.

We examined whether variation in leaf traits and thermal tolerance help maintain thermal safety margins across a wide thermal gradient. Thermal tolerance increased with MAT while predicted [?]Ttrait decreased for two of the three species. These adjustments worked together to increase both heat tolerance and avoidance in mature trees at warmer sites. This supports other studies showing that trait variation (both intra- and inter- specific) increases thermal safety margins in plants grown under warm environments compared to cooler environments (Kitudom et al., 2022; Kullberg et al., 2023; Perez & Feeley, 2020). When accounting for observed microclimate, this trait variation was not sufficient to perfectly maintain thermal safety margins but did lead to a shallower decrease in thermal safety margin with MAT than for C. sublimis which showed no variation in either [?]Ttrait or thermal tolerance. Failure to consider intraspecific trait variation in trait-based thermal safety margins may bias assessment of species vulnerability to heat stress.

Genome-wide signals of selection and genetic diversity

We hypothesised that intraspecific variation in [?]Ttrait could be explained by selection across thermal gradients. Population differentiation for most traits was stronger than expected due to genetic drift (P ST > F ST), indicating either phenotypic plasticity or divergent selection in natural populations. Genetic diversity in these species was found to be relatively low across the Wet Tropics of Queensland, with moderate-high inbreeding depression evident particularly for D. darlingiana . Although this could indicate directional selection causing the fixation of beneficial alleles or genotypes, we cannot rule out other causes such as small effective population sizes, self-pollination, or genetic drift. Our analysis revealed putative signals of selection in all species, linked to either climatic or edaphic factors. Precipitation of the driest month (Bio14) was a strong predictor of genomic variation across all species, particularly D. darlingiana and E. grandis . For these species, MAT was another key explanatory variable in the SNP-based GDMs, while soil pH was significant for C. sublimis . These species-specific differences in environmental drivers of adaptive genomic

variation were also reflected in GDMs assessing population mean leaf trait values. Climate, particularly MAT, was most influential for D. darlingiana and E. grandis, while both edaphic factors (soil pH and total soil Phosphorus) and climate were important for C. sublimis . Moisture availability and temperature are well-established drivers of mortality (Aleixo et al., 2019; Bauman, Fortunel, Delhaye, et al., 2022), growth (Bauman, Fortunel, Cernusak, et al., 2022), regeneration (Comita & Engelbrecht, 2017) and thereby species distributions (Gaviria et al., 2017) in tropical trees. The importance of edaphic variables for C. sublimis may be related to its proteoid roots (Cheesman et al., 2018), an adaptation of Proteaceae species that enhances phosphorus availability in nutrient-poor soils (Lamont, 2003). Interestingly, similar edaphic factors were not significant for D. darlingiana , also a non-mycorrhizal Proteaceae species that forms cluster roots, suggesting species-specific responses to soil conditions despite common adaptations.

Geographic distance emerged as a stronger driver of genomic variation than any single environmental variable across all species. This correlation highlights the need for caution in interpreting our results, as the adaptive signal may in part reflect neutral population structure. This aligns with evidence that functional genetic variation might be influenced by neutral processes rather than selection alone (Kardos et al., 2021; Mathur et al., 2023). Alternatively, it could indicate that loci under selection, which contribute to trait clines, may be associated with other environmental variables not explored here that correlate with geographic distance, or they may not form monotonic allele frequency clines in response to environmental gradients (Lotterhos, 2023). This does not negate the presence of adaptive signals but highlights the complexity of adaptation, driven by intricate genetic systems. Thus, our findings, while pointing to potential adaptive significance, also reflect the challenges in distinguishing selection and drift in natural populations. To address this, we complemented our field-based analyses with a genotype x environment study using climate-controlled growth chambers.

Local adaptation drives leaf thermoregulation in *E. grandis*

The implications of local adaptation from the genomic analysis were supported by the climate-controlled experiment for *E. grandis* seedlings. We found that local adaptation to MAT of origin was likely responsible for the decline in predicted $[?]T_{trait}$ with MAT across the species distribution. This was despite acclimation of some traits to temperature or VPD. Essentially, while V_{cmax25} (predicted from leaf N_{mass}) and leaf width showed plasticity to growth conditions, the net effect of this trait variation on predicted $[?]T_{trait}$ cancelled out. As a result, the variation in predicted $[?]T_{trait}$ was primarily driven through ecotypic variation in leaf width and water use efficiency. This does not mean that plasticity is unlikely to contribute to patterns of $[?]T_{trait}$ with MAT as sensitivities to covarying environmental factors may differ across species and lead to different plastic and adaptive responses (Middleby, Cheesman, Hopkinson, et al., 2024).

Across the Wet Tropics of Queensland, warmer areas are usually also wetter due to the lowlands being located along the coast and the tablelands being in a rain shadow. Trees located in warm-wet sites may benefit more from having less conservative water use strategies that maintain carbon uptake and thermal cooling compared to trees located in warm-dry sites. While our seedling provenance collection for the glasshouse experiment was guided by contrasting MAT of origin, we tested how genotype x environment effects of different growth temperatures were impacted by vapour pressure deficit. Moreover, the generalized dissimilarity modelling on outlier SNPs identified using GPA indicated that precipitation of the driest month was a more important explanatory variable than MAT. It is possible then that ecotypic variation observed in the glasshouse was driven by changes in precipitation rather than temperature, however the included provenances did not cover as even a distribution of precipitation of origin as they did for MAT of origin.

Conclusions and recommendations for future research

Our study supports growing evidence that while some tropical tree species exhibit acclimation and/or adaptation in leaf thermal traits, patterns of intraspecific variation differ across species (Blonder et al., 2020; Middleby, Cheesman, Hopkinson, et al., 2024; Tarvainen et al., 2022). Our findings indicate that limited

homeothermy is present in some, but not all, tropical tree species, and that local adaptation to climate significantly influences variation in leaf thermoregulatory traits for certain species. This underscores the importance of considering intraspecific variation in leaf thermal traits when evaluating plant responses to climate change, as it may affect the adaptive capacity and resilience of tropical rainforest trees. However, it remains unclear whether observed ecotypic variation is a response to thermal or moisture gradients, and whether leaf thermoregulation itself is under selection or if this is just a byproduct of adaptive variation to maintain carbon uptake or avoid water stress. Future research should focus on expanding studies of plant thermoregulation by leveraging existing trait- and genetic datasets to better understand vulnerability and resilience of tropical rainforest trees in the face of climate change.

Acknowledgements

We would like to sincerely thank volunteers Flossie Brown, Tombo Warra, Michael Bewley Green, Rachael Walshe, Jayden Engert, Nara Vogado, and Sebastian Garavito Ramirez for their assistance during measurement campaigns.

CRediT

KM = Conceptualisation, Investigation, Formal Analysis, Funding Acquisition, Writing – Original Draft Preparation; **RJ** = Methodology, Validation; **AC** = Conceptualisation, Investigation, Funding Acquisition; **MR** = Methodology, Resources, Validation;**LC, MB, & DC** = Supervision, Funding Acquisition; All authors contributed to Writing - Review & Editing.

Funding

Support for this research was provided by funding to KM from the Skyrail Rainforest Foundation and Holsworth Wildlife Endowment, and from the Australian Research Council (LP190100484; DP210103186).

References

https://doi.org/10.1038/s41558-019-0458-0

https://doi.org/10.1093/jxb/erz467

https://doi.org/10.1088/1748-9326/abe3b9

https://doi.org/10.1111/1365-2745.13354

https://doi.org/10.1111/gcb.15982

https://doi.org/10.1038/s41586-022-04737-7

https://doi.org/10.1111/1365-2435.13643

https://doi.org/10.1111/nph.18800

https://doi.org/10.1038/s41598-023-31711-8

https://doi.org/10.1111/1755-0998.13074

https://doi.org/10.1038/s41576-019-0152-0

https://doi.org/10.1007/s10592-012-0425-z

https://doi.org/10.5194/essd-14-5573-2022

https://doi.org/10.1093/molbev/msz008

https://doi.org/10.1111/1365-2664.12980
https://doi.org/10.1017/CBO9781107323506.013
https://doi.org/10.1111/ele.14416
https://doi.org/10.5194/bg-16-903-2019
https://doi.org/10.1038/hdy.2015.93
https://doi.org/10.1111/nph.19558
https://doi.org/10.1038/s41586-023-06391-z
https://doi.org/10.1111/nph.16733
https://doi.org/10.1111/gcb.14037
https://doi.org/10.1371/journal.pone.0143346
https://doi.org/10.1016/j.foreco.2020.118304
https://doi.org/10.1007/bf00386231
https://doi.org/10.1111/eva.13323
https://doi.org/10.1111/pce.13208
https://doi.org/10.1111/j.1472-4642.2007.00341.x
https://doi.org/10.1111/mec.14584
https://doi.org/10.1073/pnas.0904209106
https://doi.org/10.1111/2041-210x.12382
https://doi.org/10.1002/ecs2.1712
https://doi.org/10.1111/nph.18632
https://doi.org/10.1016/j.agrformet.2022.108827
https://doi.org/10.1111/jeb.13262
https://doi.org/10.1038/nature07031
https://doi.org/10.1007/s00442-018-4198-z
https://doi.org/10.1093/bioinformatics/btn129
https://doi.org/10.1017/CBO9780511845727
https://doi.org/10.1111/ele.14348
https://doi.org/10.1073/pnas.2104642118
https://doi.org/10.1038/sdata.2017.122
https://doi.org/10.1111/ecog.04680
https://doi.org/10.1111/2041-210x.12067
https://doi.org/10.1016/j.scitotenv.2021.150416
https://doi.org/10.1016/j.jplph.2013.01.005
https://doi.org/10.1111/nph.19413

https://doi.org/10.1093/treephys/tpac066

https://doi.org/10.1111/pce.12857

https://doi.org/10.1111/gcb.16711

https://doi.org/10.1371/journal.pone.0224218

https://doi.org/10.1016/j.agrformet.2007.05.007

https://doi.org/10.1111/gcb.15129

https://doi.org/10.1073/pnas.2220313120

https://doi.org/10.1111/1755-0998.12592

https://doi.org/10.1111/2041-210x.13093

https://doi.org/10.1016/0098-8472(88)90059-7

https://doi.org/10.1111/gcb.16929

https://doi.org/10.1111/geb.12972

https://doi.org/10.1111/gcb.16407

https://doi.org/10.1073/pnas.2303043120

https://doi.org/10.1111/nph.13579

https://doi.org/10.1111/j.1365-2486.2010.02375.x

https://doi.org/10.1016/j.tree.2015.09.006

https://doi.org/10.1111/nph.19822

https://doi.org/10.1111/pce.15141

https://doi.org/10.1038/s41586-018-0300-2

https://doi.org/10.1111/geb.13459

https://doi.org/https://doi.org/10.1016/B978-0-12-386910-4.00020-2

https://doi.org/10.1002/ecy.3151

https://doi.org/10.1002/ecs2.2311

https://doi.org/10.1111/1365-2435.13658

https://doi.org/10.1071/bt12225

https://doi.org/10.1371/journal.pone.0146021

https://doi.org/10.1111/rec.12898

https://doi.org/10.1104/pp.16.00476

https://doi.org/10.1186/1746-4811-6-16

https://doi.org/10.1046/j.1365-294x.1998.00334.x

https://doi.org/10.1007/s10592-015-0741-1

https://doi.org/10.1111/mec.15672

https://doi.org/10.1111/j.1469-8137.2011.03851.x

https://doi.org/10.1007/s11295-013-0596-x

https://doi.org/10.1111/mec.12751

https://doi.org/10.1073/pnas.2205682119

https://doi.org/10.1073/pnas.2302515120

https://doi.org/10.1111/nph.17809

https://doi.org/10.1111/geb.13272

https://doi.org/10.1080/15592324.2017.1356534

https://doi.org/10.1093/zoolinnean/zly007

https://doi.org/10.1002/ece3.4046

https://doi.org/10.1126/science.aal4760

https://doi.org/10.1038/nature02403

https://doi.org/10.1093/bioinformatics/bts606

https://doi.org/10.1016/j.agrformet.2023.109766

https://doi.org/10.1073/pnas.0901643106

Aleixo, I., Norris, D., Hemerik, L., Barbosa, A., Prata, E., Costa, F., & Poorter, L. (2019). Amazonian rainforest tree mortality driven by climate and functional traits. *Nature Climate Change* , *9* , 384-388. Arab, M. M., Marrano, A., Abdollahi-Arpanahi, R., Leslie, C. A., Cheng, H., Neale, D. B., & Vahdati, K. (2020). Combining phenotype, genotype, and environment to uncover genetic components underlying water use efficiency in Persian walnut. *Journal of Experimental Botany* ,*71* (3), 1107-1127. Araujo, I., Marimon, B. S., Scalon, M. C., Fauset, S., Junior, B. M., Tiwari, R. et al. (2021). Trees at the Amazonia-Cerrado transition are approaching high temperature thresholds.*Environmental Research Letters* , *16* (3), 7, Article 034047. Barton, K. E., Jones, C., Edwards, K. F., Shiels, A. B., & Knight, T. (2020). Local adaptation constrains drought tolerance in a tropical foundation tree. *Journal of Ecology* , *108* (4), 1540-1552. Bauman, D., Fortunel, C., Cernusak, L. A., Bentley, L. P., Mcmahon, S. M., Rifai, S. W. et al. (2022). Tropical tree growth sensitivity to climate is driven by species intrinsic growth rate and leaf traits.*Global Change Biology* , *28* (4), 1414-1432. Bauman, D., Fortunel, C., Delhaye, G., Malhi, Y., Cernusak, L. A., Bentley, L. P. et al. (2022). Tropical tree mortality has increased with rising atmospheric water stress. *Nature* , *608* (7923), 528-533. Blonder, B., Escobar, S., Kapas, R. E., & Michaletz, S. T. (2020). Low predictability of energy balance traits and leaf temperature metrics in desert, montane and alpine plant communities. *Functional Ecology* ,*34* (9), 1882-1897. Blonder, B. W., Aparecido, L. M. T., Hultine, K. R., Lombardozzi, D., Michaletz, S. T., Posch, B. C. et al. (2023). Plant water use theory should incorporate hypotheses about extreme environments, population ecology, and community ecology. *New Phytologist* , *238* (6), 2271-2283. Botta-Dukat, Z. (2023). Quartile coefficient of variation is more robust than CV for traits calculated as a ratio. *Scientific Reports* , *13* (1). Bragg, J. G., Cuneo, P., Sherieff, A., & Rossetto, M. (2020). Optimizing the genetic composition of a translocation population: Incorporating constraints and conflicting objectives. *Molecular Ecology Resources* ,*20* (1), 54-65. Breed, M. F., Harrison, P. A., Blyth, C., Byrne, M., Gaget, V., Gellie, N. J. C. et al. (2019). The potential of genomics for restoring ecosystems and biodiversity. *Nature Reviews Genetics* , *20* (10), 615-628. Breed, M. F., Stead, M. G., Ottewell, K. M., Gardner, M. G., & Lowe, A. J. (2013). Which provenance and where? Seed sourcing strategies for revegetation in a changing environment. *Conservation Genetics* , *14* (1), 1-10. Brun, P., Zimmermann, N. E., Hari, C., Pellissier, L., & Karger, D. N. (2022). Global climate-related predictors at kilometer resolution for the past and future. *Earth System Science Data* , *14* (12), 5573-5603. Campbell, G. S., & Norman, J. M. (1998). *Introduction to environmental biophysics, 2^{nd} edition. Springer* . New York, NY. https://doi.org/10.1007/978-1-4612-1626-1Caye, K., Jumentier, B., Lepeule, J., & Francois, O. (2019). LFMM 2: Fast and Accurate Inference

of Gene-Environment Associations in Genome-Wide Studies.*Molecular Biology and Evolution* , *36* (4), 852-860. Cheesman, A. W., Preece, N. D., van Oosterzee, P., Erskine, P. D., & Cernusak, L. A. (2018). The role of topography and plant functional traits in determining tropical reforestation success. *Journal of Applied Ecology* , *55* (2), 1029-1039. Comita, L. S., & Engelbrecht, B. M. J. (2017). Drought as a driver of tropical tree species regeneration dynamics and distribution patterns. In D. A. Coomes, D. Burslem, & W. D. Simonson (Eds.), *Forests and Global Change* (pp. 261-308). Cambridge University Press. Cook, A. M., Rezende, E. L., Petrou, K., & Leigh, A. (2024). Beyond a single temperature threshold: Applying a cumulative thermal stress framework to plant heat tolerance.*Ecology Letters* , *27* (3). De Kauwe, M. G., Medlyn, B. E., Pitman, A. J., Drake, J. E., Ukkola, A., Griebel, A., et al. (2019). Examining the evidence for decoupling between photosynthesis and transpiration during heat extremes. *Biogeosciences* , *16* (4), 903-916. de Villemereuil, P., Gaggiotti, O. E., Mouterde, M., & Till-Bottraud, I. (2016). Common garden experiments in the genomic era: new perspectives and opportunities. *Heredity* , *116* (3), 249-254. Diao, H., Cernusak, L. A., Saurer, M., Gessler, A., Siegwolf, R. T. W., & Lehmann, M. M. (2024). Uncoupling of stomatal conductance and photosynthesis at high temperatures: mechanistic insights from online stable isotope techniques. *New Phytologist* . Doughty, C. E., Keany, J. M., Wiebe, B. C., Rey-Sanchez, C., Carter, K. R., Middleby, K. B., et al. B. (2023). Tropical forests are approaching critical temperature thresholds. *Nature* . Drake, J. E., Harwood, R., Varhammar, A., Barbour, M. M., Reich, P. B., Barton, C. V. M., & Tjoelker, M. G. (2020). No evidence of homeostatic regulation of leaf temperature inEucalyptus parramattensistrees: integration of CO(2) flux and oxygen isotope methodologies. *New Phytologist* , *228* (5), 1511-1523. Drake, J. E., Tjoelker, M. G., Varhammar, A., Medlyn, B. E., Reich, P. B., Leigh, A., et al. (2018). Trees tolerate an extreme heatwave via sustained transpirational cooling and increased leaf thermal tolerance. *Global Change Biology* , *24* (6), 2390-2402. Duursma, R. A. (2015). Plantecophys - An R Package for Analysing and Modelling Leaf Gas Exchange Data. *Plos One* ,*10* (11), 13, Article e0143346. Engert, J. E., Vogado, N. O., Freebody, K., Byrne, B., Murphy, J., Sheather, G., et al. (2020). Functional trait representation differs between restoration plantings and mature tropical rainforest. *Forest Ecology and Management* ,*473* , 9, Article 118304. Farquhar, G. D., Caemmerer, S. V., & Berry, J. A. (1980). A biochemical-model of photosynthetic CO2 assimilation in leaves of C-3 species. *Planta* , *149* (1), 78-90. Faske, T. M., Agneray, A. C., Jahner, J. P., Sheta, L. M., Leger, E. A., & Parchman, T. L. (2021). Genomic and common garden approaches yield complementary results for quantifying environmental drivers of local adaptation in rubber rabbitbrush, a foundational Great Basin shrub. *Evolutionary Applications* , *14* (12), 2881-2900. Fauset, S., Freitas, H. C., Galbraith, D. R., Sullivan, M. J. P., Aidar, M. P. M., Joly, C. A., et al. (2018). Differences in leaf thermoregulation and water use strategies between three co-occurring Atlantic forest tree species. *Plant Cell and Environment* ,*41* (7), 1618-1631. Ferrier, S., Manion, G., Elith, J., & Richardson, K. (2007). Using generalized dissimilarity modelling to analyse and predict patterns of beta diversity in regional biodiversity assessment. *Diversity and Distributions* , *13* (3), 252-264. Forester, B. R., Lasky, J. R., Wagner, H. H., & Urban, D. L. (2018). Comparing methods for detecting multilocus adaptation with multivariate genotype-environment associations. *Molecular Ecology* ,*27* (9), 2215-2233. Franks, P. J., & Beerling, D. J. (2009). Maximum leaf conductance driven by CO2 effects on stomatal size and density over geologic time. *Proceedings of the National Academy of Sciences* , *106* (25), 10343-10347. Frichot, E., & Francois, O. (2015). LEA: An R package for landscape and ecological association studies. *Methods in Ecology and Evolution* , *6* (8), 925-929. Gaviria, J., Turner, B., & Engelbrecht, B. (2017). Drivers of tree species distribution across a tropical rainfall gradient.*ECOSPHERE* , *8* , Article e01712. Geange, S. R., Arnold, P. A., Catling, A. A., Coast, O., Cook, A. M., Gowland, K. M., et al. (2021). The thermal tolerance of photosynthetic tissues: a global systematic review and agenda for future research. *New Phytologist* , 229, 2497-2513. https://doi.org/10.1111/nph.17052Guo, Z., Still, C. J., Lee, C. K. F., Ryu, Y., Blonder, B., Wang, J., et al. (2023). Does plant ecosystem thermoregulation occur? An extratropical assessment at different spatial and temporal scales. *New Phytologist* , *238* (3), 1004-1018. Guo, Z. F., Yan, Z. B., Majcher, B. M., Lee, C. K. F., Zhao, Y. Y., Song, G. Q., et al. (2022). Dynamic biotic controls of leaf thermoregulation across the diel timescale.*Agricultural and Forest Meteorology* , *315* , 11, Article 108827. Halbritter, A. H., Fior, S., Keller, I., Billeter, R., Edwards, P. J., Holderegger, R., et al. (2018). Trait differentiation and adaptation of plants along elevation gradients. *Journal of Evolutionary Biology* , *31* (6), 784-800. Helliker,

B. R., & Richter, S. L. (2008). Subtropical to boreal convergence of tree-leaf temperatures. *Nature* , *454* (7203), 511-U516. Helliker, B. R., Song, X., Goulden, M. L., Clark, K., Bolstad, P., Munger, J. W. et al. (2018). Assessing the interplay between canopy energy balance and photosynthesis with cellulose delta O-18: large-scale patterns and independent ground-truthing. *Oecologia* , *187* (4), 995-1007. Hijmans, R. (2022). raster: Geographic Data Analysis and Modeling. In (Vol. R package version 3.6-11).IPCC. (2022). *Climate Change 2022: Impacts, Adaptation, and Vulnerability* (Contribution of Working Group II to the Sixth Assessment Report of the Intergovernmental Panel on Climate Change [H.-O. Portner, D.C. Roberts, M. Tignor, E.S. Poloczanska, K. Mintenbeck, A. Alegria, M. Craig, S. Langsdorf, S. Loschke, V. Moller, A. Okem, B. Rama (eds.)]. , Issue. Jombart, T. (2008). adegenet: a R package for the multivariate analysis of genetic markers. *Bioinformatics* , *24* (11), 1403-1405. Jones, H. G. (2013). *Plants and Microclimate: A Quantitative Approach to Environmental Plant Physiology* (3 ed.). Cambridge University Press. Jordan, R., Harrison, P. A., & Breed, M. (2024). The eco-evolutionary risks of not changing seed provenancing practices in changing environments. *Ecology Letters* , *27* (1). Kardos, M., Armstrong, E. E., Fitzpatrick, S. W., Hauser, S., Hedrick, P. W., Miller, J. M. et al. (2021). The crucial role of genome-wide genetic variation in conservation. *Proceedings of the National Academy of Sciences* , *118* (48), e2104642118. Karger, D. N., Conrad, O., Bohner, J., Kawohl, T., Kreft, H., Soria-Auza, R. W., et al. (2017). Climatologies at high resolution for the earth's land surface areas.*Scientific Data* , *4* (1), 170122. Kearney, M. R., & Porter, W. P. (2020). NicheMapR - an R package for biophysical modelling: the ectotherm and Dynamic Energy Budget models. *Ecography* ,*43* (1), 85-96. Keenan, K., Mcginnity, P., Cross, T. F., Crozier, W. W., & Prodohl, P. A. (2013). diveRsity: An R package for the estimation and exploration of population genetics parameters and their associated errors. *Methods in Ecology and Evolution* , *4* (8), 782-788. Kelly, J. W. (2014). *Productivity and water use of Australian tree species under climate change* . Macquarie University. Thesis. https://doi.org/10.25949/19444616.v1Kitudom, N., Fauset, S., Zhou, Y. Y., Fan, Z. X., Li, M. R., He, M. J. et al. (2022). Thermal safety margins of plant leaves across biomes under a heatwave.*Science of the Total Environment* , *806* , Article 150416. Krause, G. H., Cheesman, A. W., Winter, K., Krause, B., & Virgo, A. (2013). Thermal tolerance, net CO2 exchange and growth of a tropical tree species, Ficus insipida, cultivated at elevated daytime and nighttime temperatures. *Journal of Plant Physiology* ,*170* (9), 822-827. Kullberg, A. T., Coombs, L., Soria Ahuanari, R. D., Fortier, R. P., & Feeley, K. J. (2023). Leaf thermal safety margins decline at hotter temperatures in a natural warming 'experiment' in the Amazon. *New Phytologist* . Kullberg, A. T., & Feeley, K. J. (2022). Limited acclimation of leaf traits and leaf temperatures in a subtropical urban heat island. *Tree Physiology* . Lamont, B. (2003). Structure, ecology and physiology of root clusters - a review.*Plant and Soil* , *248* , 1-19. https://doi.org/10.1023/A:1022314613217Leigh, A., Sevanto, S., Close, J. D., & Nicotra, A. B. (2017). The influence of leaf size and shape on leaf thermal dynamics: does theory hold up under natural conditions?.*Plant Cell and Environment* , *40* (2), 237-248. Leites, L., & Garzon, B., Marta. (2023). Forest tree species adaptation to climate across biomes: Building on the legacy of ecological genetics to anticipate responses to climate change. *Global Change Biology* ,*29* (17), 4711-4730. Leon-Garcia, I. V., & Lasso, E. (2019). High heat tolerance in plants from the Andean highlands: Implications for paramos in a warmer world. *Plos One* , *14* (11), Article e0224218. Leuzinger, S., & Korner, C. (2007). Tree species diversity affects canopy leaf temperatures in a mature temperate forest.*Agricultural and Forest Meteorology* , *146* (1-2), 29-37. Liancourt, P., Song, X., Macek, M., Santrucek, J., & Dolezal, J. (2020). Plant's-eye view of temperature governs elevational distributions. *Global Change Biology* , *26* (7), 4094-4103. Lotterhos, K. (2023). The paradox of adaptive trait clines with nonclinal patterns in the underlying genes. *PNAS* , *120* , Article e2220313120. Luu, K., Bazin, E., & Blum, M. G. B. (2017). pcadapt: an R package to perform genome scans for selection based on principal component analysis. *Molecular Ecology Resources* ,*17* (1), 67-77. Maclean, I. M. D., Mosedale, J. R., & Bennie, J. J. (2019). Microclima: An r package for modelling meso- and microclimate. *Methods in Ecology and Evolution* , *10* (2), 280-290. Mahan, J. R., & Upchurch, D. R. (1988). MAINTENANCE OF CONSTANT LEAF TEMPERATURE BY PLANTS .1. HYPOTHESIS LIMITED HOMEOTHERMY.*Environmental and Experimental Botany* , *28* (4), 351-357. Marchin, R. M., Medlyn, B. E., Tjoelker, M. G., & Ellsworth, D. S. (2023). Decoupling between stomatal conductance and photosynthesis occurs under extreme heat in broadleaf tree species regardless of water access. *Global Change Biology* , *29* (22), 6319-6335. Matesanz, S., & Ramirez-Valiente, J. A. (2019). A

review and meta-analysis of intraspecific differences in phenotypic plasticity: Implications to forecast plant responses to climate change. *Global Ecology and Biogeography* , *28* (11), 1682-1694. Mathias, J., & Hudiburg, T. (2022). isocalcR: An R package to streamline and standardize stable isotope calculations in ecological research.*Global Change Biology* , *28* , 7428-7436. Mathur, S., Mason, A., Bradburd, G., & Gibbs, L. (2023). Functional genomic diversity is correlated with neutral genomic diversity in populations of an endangered rattlesnake. *PNAS* , *120* , Article e2303043120. Mcelwain, J. C., Yiotis, C., & Lawson, T. (2016). Using modern plant trait relationships between observed and theoretical maximum stomatal conductance and vein density to examine patterns of plant macroevolution. *New Phytologist* , *209* (1), 94-103. Medlyn, B. E., Duursma, R. A., Eamus, D., Ellsworth, D. S., Prentice, I. C., Barton, C. V. M., et al. (2011). Reconciling the optimal and empirical approaches to modelling stomatal conductance. *Global Change Biology* , *17* (6), 2134-2144. Michaletz, S. T., Weiser, M. D., Zhou, J. Z., Kaspari, M., Helliker, B. R., & Enquist, B. J. (2015). Plant Thermoregulation: Energetics, Trait-Environment Interactions, and Carbon Economics. *Trends in Ecology & Evolution* , *30* (12), 714-724. Middleby, K. B., Cheesman, A. W., & Cernusak, L. A. (2024). Impacts of elevated temperature and vapour pressure deficit on leaf gas exchange and plant growth across six tropical rainforest tree species.*New Phytologist* . Middleby, K. B., Cheesman, A. W., Hopkinson, R., Baker, L., Ramirez Garavito, S., Breed, M. F., & Cernusak, L. A. (2024). Ecotypic Variation in Leaf Thermoregulation and Heat Tolerance but Not Thermal Safety Margins in Tropical Trees. *Plant, Cell & Environment* . Mitchard, E. T. A. (2018). The tropical forest carbon cycle and climate change. *Nature* , *559* (7715), 527-534. Mokany, K., Ware, C., Woolley, S. N. C., Ferrier, S., & Fitzpatrick, C., Matthew. (2022). A working guide to harnessing generalized dissimilarity modelling for biodiversity analysis and conservation assessment. *Global Ecology and Biogeography* , *31* (4), 802-821. Monteith, J., & Unsworth, M. (2013). *Principles of Environmental Physics* (4 ed.). Academic Press. . Muehleisen, A. J., Engelbrecht, B. M. J., Jones, F. A., Manzane-Pinzon, E., & Comita, L. S. (2020). Local adaptation to herbivory within tropical tree species along a rainfall gradient. *Ecology* , *101* (11), 10. Oksanen, J., Simpson, G., Blanchet, F., Kindt, R., Legendre, P., Minchin, P., & al., e. (2022). vegan: Community Ecology Package. In (Vol. R package version 2.6-4).Pau, S., Detto, M., Kim, Y., & Still, C. J. (2018). Tropical forest temperature thresholds for gross primary productivity.*Ecosphere* , *9* (7), Article e02311. Perez, T. M., & Feeley, K. J. (2020). Photosynthetic heat tolerances and extreme leaf temperatures. *Functional Ecology* , *34* (11), 2236-2245. Perez-Harguindeguy, N., Diaz, S., Garnier, E., Lavorel, S., Poorter, H., Jaureguiberry, P., et al. (2013). New handbook for standardised measurement of plant functional traits worldwide. *Australian Journal of Botany* , *61* (3), 167-234. Ritz, C., Baty, F., Streibig, J. C., & Gerhard, D. (2015). Dose-Response Analysis Using R. *PLOS ONE* , *10* (12), e0146021. Rossetto, M., Bragg, J., Kilian, A., McPherson, H., van der Merwe, M., & Wilson, P. D. (2019). Restore and Renew: a genomics-era framework for species provenance delimitation.*Restoration Ecology* , *27* (3), 538-548. Sack, L., & Buckley, T. (2016). The Developmental Basis of Stomatal Density and Flux.*Plant Physiology* , *171* , 2358-2363. Sansaloni, C. P., Petroli, C. D., Carling, J., Hudson, C. J., Steane, D. A., Myburg, A. A., et al. (2010). A high-density Diversity Arrays Technology (DArT) microarray for genome-wide genotyping in *Eucalyptus* . *Plant Methods* , *6* , Article 16. Schneider, C. J., Cunningham, M., & Moritz, C. (1998). Comparative phylogeography and the history of endemic vertebrates in the Wet Tropics rainforests of Australia. *Molecular Ecology* , *7* (4), 487-498. Shryock, D. F., Havrilla, C. A., Defalco, L. A., Esque, T. C., Custer, N. A., & Wood, T. E. (2015). Landscape genomics of Sphaeralcea ambigua in the Mojave Desert: a multivariate, spatially-explicit approach to guide ecological restoration. *Conservation Genetics* , *16* (6), 1303-1317. Shryock, D. F., Washburn, L. K., DeFalco, L. A., & Esque, T. C. (2021). Harnessing landscape genomics to identify future climate resilient genotypes in a desert annual. *Molecular Ecology* , 20. Song, X., Barbour, M. M., Saurer, M., & Helliker, B. R. (2011). Examining the large-scale convergence of photosynthesis-weighted tree leaf temperatures through stable oxygen isotope analysis of multiple data sets. *New Phytologist* , *192* (4), 912-924. Sork, V. L., Aitken, S. N., Dyer, R. J., Eckert, A. J., Legendre, P., & Neale, D. B. (2013). Putting the landscape into the genomics of trees: approaches for understanding local adaptation and population responses to changing climate. *Tree Genetics & Genomes* , *9* (4), 901-911. Steane, D. A., Potts, B. M., McLean, E., Prober, S. M., Stock, W. D., Vaillancourt, R. E., & Byrne, M. (2014). Genome-wide scans detect adaptation to aridity in a widespread forest tree species.*Molecular Ecology* , *23* (10), 2500-2513. Still, C. J., Page, G., Rastogi, B., Griffith, D. M.,

Aubrecht, D. M., Kim, Y. et al. (2022). No evidence of canopy-scale leaf thermoregulation to cool leaves below air temperature across a range of forest ecosystems. *PNAS* ,*119* (38). Still, C. J., Page, G. F. M., Rastogi, B., Griffith, D. M., Aubrecht, D. M., Kim, Y., et al. (2023). Reply to Garen et al.: Within-canopy temperature data also do not support limited homeothermy.*Proceedings of the National Academy of Sciences* , *120* (15). Tarvainen, L., Wittemann, M., Mujawamariya, M., Manishimwe, A., Zibera, E., Ntirugulirwa, B., et al. (2022). Handling the heat – photosynthetic thermal stress in tropical trees. *New Phytologist* , *233* (1), 236-250. Trew, B. T., & Maclean, I. M. D. (2021). Vulnerability of global biodiversity hotspots to climate change. *Global Ecology and Biogeography* , *30* (4), 768-783. UNESCO World Heritage Centre (1988). Inscription: Wet Tropics of Queensland (Australia). In *World Heritage List* . Urban, J., Ingwers, M., McGuire, M. A., & Teskey, R. O. (2017). Stomatal conductance increases with rising temperature. *Plant Signaling & Behavior* , *12* (8), 3, Article e1356534. Weigand, H., & Leese, F. (2018). Detecting signatures of positive selection in non-model species using genomic data.*Zoological Journal of the Linnean Society* , *184* (2), 528-583. Weir, B. S., & Hill, W. G. (2002). Estimating F-statistics. In (Vol. 36, pp. 721-750): Annu. Rev. Genet.Woods, H. A., Saudreau, M., & Pincebourde, S. (2018). Structure is more important than physiology for estimating intracanopy distributions of leaf temperatures. *Ecology and Evolution* , *8* (10), 5206-5218. Wright, I. J., Dong, N., Maire, V., Prentice, I. C., Westoby, M., Diaz, S., et al. (2017). Global climatic drivers of leaf size. *Science* , *357* (6354), 917-+. Wright, I. J., Reich, P. B., Westoby, M., Ackerly, D. D., Baruch, Z., Bongers, F. et al. (2004). The worldwide leaf economics spectrum.*Nature* , *428* (6985), 821-827. Zheng, X., Levine, D., Shen, J., Gogarten, S. M., Laurie, C., & Weir, B. S. (2012). A high-performance computing toolset for relatedness and principal component analysis of SNP data. *Bioinformatics* , *28* (24), 3326-3328. Zhou, Y. Y., Kitudom, N., Fauset, S., Slot, M., Fan, Z. X., Wang, J. P. et al. (2023). Leaf thermal regulation strategies of canopy species across four vegetation types along a temperature and precipitation gradient. *Agricultural and Forest Meteorology* ,*343* , Article 109766. Zimmermann, N. E., Yoccoz, N. G., Edwards, T. C., Meier, E. S., Thuiller, W., Guisan, A., et al (2009). Climatic extremes improve predictions of spatial patterns of tree species.*PNAS, 106* , 19723-19728.

Supplementary Materials

Method S1: Extended method descriptions from field measurements

Leaf spectra

Reflectance and transmittance spectra from wavelengths 390-1100 nm were collected for the adaxial side of leaves using a spectrometer (Jaz Spectrometer, Ocean Optics, Ocean Insight, Orlando, FL, US) and external type integrating sphere with a halogen light source 'illuminator' (LI-1800-12, LI-COR Biosciences, Lincoln, NE, US). Spectra were obtained using the 'OceanView' software (Ocean Optics, Ocean Insight, Orlando, FL, US). The scanning parameters were set to average 40 scans with a boxcar width of 5, nonlinearity correction enabled, and default settings for integrating time. Barium sulphate was used as reference material. For each leaf, reflectance and transmittance sample and reference measurements were taken, with a dark reference collected every 10-15 minutes. Absorptance was then calculated using the formula: Absorptance = 1 – Reflectance – Transmittance.

Stomatal anatomy

Leaf stomatal imprints were obtained on 3 leaves per plant using nail varnish and tape on the abaxial mid-lamina. Stomatal imprints for*C. sublimis* were impacted by leaf hairs so stomatal anatomical traits are only presented for *E. grandis* and *D. darlingiana* . Microscope images were obtained at x20 magnification and were processed using imageJ to obtain stomatal density (d , pores mm^{-2}), as well as stomatal length (µm) on 10 stomata per leaf. Stomatal length was converted to size (s , µm^2) assuming stomatal width is 0.5×stomatal length. Maximum theoretical conductance ($g_{\max}$, mol m^{-2} s^{-1}) was calculated as a function of

stomatal size and density as per (Franks & Beerling, 2009; Mcelwain et al., 2016; Sack & Buckley, 2016);

$$g_{\max} = \text{bmds}^{0.5}$$

where b is a biophysical constant equal to D (diffusivity of water vapour in air, $m^2\ s^{-1}$) $/v$ (molar volume of air, $m^3 mol^{-1}$) and m is a morphological constant that represents the allometric relationships between pore length and depth, and stomatal length and width. Here we used scaling factors assuming kidney bean-shaped guard cells, and as such $m = 0.432$. For$b$ factors were calculated assuming an air temperature of 25°C so that $D = 0.0000249\ m^2\ s^{-1}$ and$v = 0.0224\ m^3\ mol^{-1}$. Thereby $g_{\max}$ accounts for variation in stomatal anatomy, and not in the increase in diffusivity of water as temperature increases.

Stomatal conductance modelling

To obtain g_s, traits that impact gas exchange are required, such as the maximum rate of carboxylation (V_{cmax25}) and light-saturated rate of electron transport (J_{max25}), as well as the slope parameter (g_1) that describes the relationship between photosynthesis and stomatal conductance and responses to changes in VPD (Medlyn et al., 2011). Since characterizing V_{cmax25}, J_{max25} and g_1 in the field for each tree was not feasible, we varied these according to observed relationships with leaf N_{mass} (V_{cmax25}), and as a ratio of V_{cmax25} (J_{max}) (Figure S 8) and used thermal sensitivity of V_{cmax} and J_{max} parameters determined in Australian tropical trees (Kelly, 2014). The parameter g_1 was calculated using the following equation (Medlyn et al., 2011):

$$g_1 = \frac{(\frac{C_i}{C_a}\sqrt{\text{VPD}})}{(1 - \frac{C_i}{C_a})}$$

where VPD is the tree-level mean daytime vapour pressure deficit (kPa), and C_i/C_a is the ratio of intercellular to ambient CO_2 concentrations, estimated from leaf $\delta^{13}C$ using the 'isocalcr' package in R (Mathias & Hudiburg, 2022).

An assumption of the USO model used to predict $g_s$is that plants maximize carbon gain while minimizing water loss. This model effectively captures dynamic gas exchange and produces realistic leaf temperatures under non-stressful conditions (Guo et al., 2022). However, evidence suggests that at higher temperatures,g_s and photosynthesis decouple, withg_s maintained or even increasing (De Kauwe et al., 2019; Diao et al., 2024; Drake et al., 2018; Marchin et al., 2023; Urban et al., 2017). This decoupling may reflect a strategy to enhance transpirational cooling rather than optimizing carbon gain, especially under heat stress. Relying solely on the USO model could thus overlook plant responses aimed at maintaining T_{leaf} within a viable range. In addition, our parameterisation relies on a within-species correlation between V_{cmax25} and leaf N_{mass} that was only determined in *E. grandis* . To address these assumptions, we also calculated [?]$T_{trait}$and [?]T_{clim} using theoretical $g_{\max}$determined from stomatal anatomy, via the *findTleaf* function, which estimates T_{leaf} independently of photosynthesis. By incorporating $g_{\max}$, we aim to account for the upper limits of stomatal conductance that plants may employ in response to heat stress.

Method S2: Extended method descriptions from climate-controlled glasshouse trial

Gas exchange measurements Photosynthesis-CO2 response curves (A-Ci) were conducted using a portable gas exchange system (LiCor 6400xt; LiCor Inc., Lincoln, NE, USA) to determine Vcmax25 and Jmax25 for comparison with leaf Nitrogen content (described below). Measurements were conducted on 6 plants per chamber (8 for the warm-humid) representing one unique mother tree per plant. The cuvette conditions were conducted under ambient midday treatment temperatures (32°C for the two warm chambers, and 29°C for the cool chamber), with a flow rate of 500 µmol s-1, a PAR of 1000 µmol m-2 s-1, and an RH in the

reference air stream of 73%. The Photosyn function in the 'plantecophys' package was used to fit Vcmax and Jmax standardized to 25°C using temperature response parameters from Kelly (2014).

Leaf traits Upon completion, leaf traits (leaf width, leaf area, and fresh and dry leaf mass) were measured on 10 healthy, new, full expanded leaves per plant, including those measured for gas exchange, using standard techniques (Perez-Harguindeguy et al., 2013). The leaf material was oven-dried at 70°C for 3 days and ground for analysis of leaf δ13C and % Nitrogen. These traits were compared with observed measurements of g 1 and Vcmax25 to assess assumptions used for leaf energy balance modelling in the field campaign data. To convert δ13C values to estimates of g 1 in the glasshouse, we assumed a value of -10δ13C of CO2 in air in the glasshouse chambers.

T_{leaf} parameterisation

We estimated [?]T_{trait} for plants in the glasshouse experiment using the same leaf energy balance modelling approach as for the field campaign, with leaf traits varying by individual, and microclimate inputs standardised across all individuals to isolate the effect of trait variation on [?]T_{trait}. Microclimate inputs were T_{air} = 25°C, VPD = 1.4 kPa, PPFD = 1400 μmol m^{-2} s^{-1} and Wind = 0.5 m s^{-1}. Leaf trait inputs included leaf width, V_{cmax25} calculated from the observed relationship between Leaf N %, and g_1 calculated from leaf $\delta^{13}C$.

Table S1. Glasshouse conditions and licor set points. Values are means ± 1 SD. Mean glasshouse conditions are based on data from 9:00 to 15:00, whereas means for gas exchange survey are from licor measurements. Licor set points represent T_{leaf}, VPD_{leaf} and RH_{sample}.

	Tair (°C)	**VPD (kPa)**	**RH (%)**			
	Mean	**SD**	**Mean**	**SD**	**Mean**	**SD**
Daytime mean glasshouse conditions						
Cool-humid	25.7	1.67	1.0	0.21	71.1	4.76
Warm-humid	31.6	1.68	1.1	0.20	76.2	3.21
Warm-dry	31.7	1.70	2.0	0.45	58.7	7.02
Total 24 hour mean glasshouse conditions						
Cool-humid	21.5	3.63	0.6	0.27	76.5	5.51
Warm-humid	27.3	3.69	0.8	0.29	78.7	3.99
Warm-dry	27.4	3.70	1.2	0.67	70.4	11.31
Set points for gas exchange survey						
Cool-humid	28.9	1.69	1.2	0.19	75.7	3.98
Warm-humid	32.1	1.27	1.5	0.28	75.3	4.75
Warm-dry	32.7	1.51	1.5	0.50	77.6	4.52

Table S2. Population effects on trait variation. For each species we report the overall trait mean, along with the model results for the linear regression with population as the independent variable. Tests with $P < 0.05$ are bolded.

Trait	*Cardwellia Sublimis*	*Darlingia Darlingiana*	*Elaeocarpus Grandis*			
	Mean	R^2	**df**	**F**	P	**Mean**
LMA	137	0.36	14, 91	3.6	**< 0.0001**	169
LDMC	410	0.43	14, 91	4.98	**< 0.0001**	456
Thickness	26.34	0.8	14, 91	26.37	**< 0.0001**	34.5
Width	5.66	0.39	14, 91	4.16	**< 0.0001**	5.55
Abs	0.56	0.41	14, 90	4.42	**< 0.0001**	0.55
Ref	0.25	0.5	14, 90	6.46	**< 0.0001**	0.27

Trait	*Cardwellia Sublimis*	*Darlingia Darlingiana*	*Elaeocarpus Grandis*			
N %	0.95	0.23	14, 91	1.94	**0.0324**	0.98
C/N ratio	47.4	0.15	14, 91	1.14	0.339	48.91
δ^{13}	-28.9	0.1	14, 91	0.72	0.752	-30.7
g_1	3.18	0.21	14, 91	1.68	0.0731	5.71
Stomatal density	NA	NA	NA	NA	NA	335
Stomatal size	NA	NA	NA	NA	NA	429
g_{max}	NA	NA	NA	NA	NA	3.3
$\mathbf{T_{crit}}$	44.26	0.4	3, 17	3.83	**0.0291**	45.12
$\mathbf{T_{50}}$	49.46	0.3	3, 17	2.38	0.105	49.68
$\mathbf{[?]T_{trait}}$	5.95	0.37	14, 90	3.83	$<$ **0.0001**	5.06
Anatomical $\mathbf{[?]T_{trait}}$	NA	NA	NA	NA	NA	-0.63
$\mathbf{TSM_{trait}}$	18.71	0.31	3, 17	2.56	0.0893	19.75
Anatomical $\mathbf{TSM_{trait}}$	NA	NA	NA	NA	NA	25.88

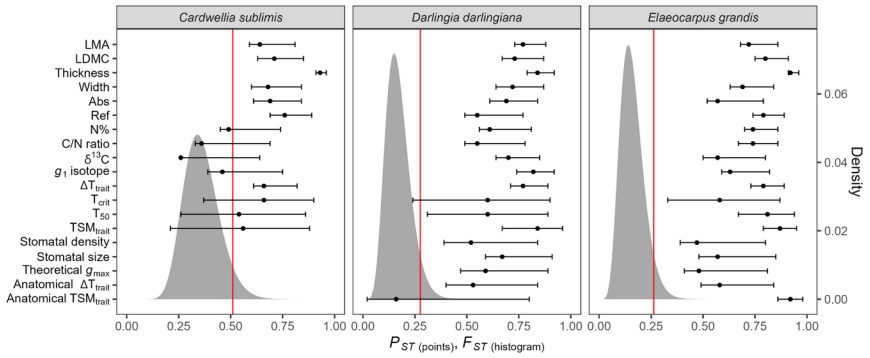

Figure S1. Comparison of observed trait differentiation (PST) and expected neutral divergence (FST) across species and traits. The black points represent PST values for individual traits, with error bars showing the 95% confidence intervals from 1000 bootstrapped replicates. Dark grey shading represents the $\chi 2$ distribution of FST estimates for each species and red vertical lines indicate the 5% upper limit of the FST estimates (empirical 95% cut-off) to test for significant differentiation beyond neutral expectations. Overall FST estimated from analysis of molecular variance on all SNPs using the 'poppr' package.

Table S3. Mean annual temperature effects on trait variation. For each species we report the slope estimate, along with model results for the linear regression with mean annual temperature as the independent variable. Tests with P $<$ 0.05 are bolded.

Trait	*Cardwellia sublimis*	*Darlingia darlingiana*	*Elaeocarpus grandis*				
	Slope	**df**	**F**	*P*	**Slope**	**df**	**F**
LMA	0.6	1, 104	0.292	0.59	-6.84	1, 94	4
LDMC	3.23	1, 104	3.228	0.0753	-1.44	1, 94	0
Thickness	-0.04	1, 104	0.031	0.86	-0.7	1, 94	6
Width	0.05	1, 104	1.069	0.303	0.14	1, 94	1
Abs	0	1, 103	0.205	0.652	0	1, 94	4
Ref	0	1, 103	3.761	0.0552	0	1, 94	0
N %	-0.01	1, 104	3.26	0.0739	0	1, 94	0

Trait	*Cardwellia sublimis*	*Darlingia darlingiana*	*Elaeocarpus grandis*				
C/N ratio	0.46	1, 104	1.417	0.237	0.03	1, 94	0.
δ^{13}	-0.01	1, 104	0.042	0.837	-0.31	1, 94	4
g_1	0.13	1, 104	15.619	**0.0001**	0.86	1, 94	7
Stomatal density	NA	NA	NA	NA	2.65	1, 33	0.
Stomatal size	NA	NA	NA	NA	-4.86	1, 33	0.
$g_{\mathbf{max}}$	NA	NA	NA	NA	0.02	1, 33	0.
$\mathbf{T_{crit}}$	0.14	1, 19	0.172	0.683	0.27	1, 20	0.
$\mathbf{T_{50}}$	0.01	1, 19	0.005	0.945	0.22	1, 20	4.
$\mathbf{[?]T_{trait}}$	-0.02	1, 103	0.559	0.457	-0.21	1, 94	5
Anatomical $\mathbf{[?]T_{trait}}$	NA	NA	NA	NA	0.02	1, 33	0.
$\mathbf{TSM_{trait}}$	0.03	1, 19	0.092	0.765	0.52	1, 20	3
Anatomical $\mathbf{TSM_{trait}}$	NA	NA	NA	NA	0.09	1, 9	0.

Note: LMA = leaf mass per area, LDMC = leaf dry matter content, Abs = Absorptance, Ref = Reflectance, N % = % leaf Nitrogen, C/N ratio = Carbon/Nitrogen ratio, g_1 = stomatal slope parameter, g_{max} = theoretical maximum conductance, $[?]T_{trait}$ = leaf-air temperature calculated using tree-level traits, and TSM_{trait} = thermal safety margin.

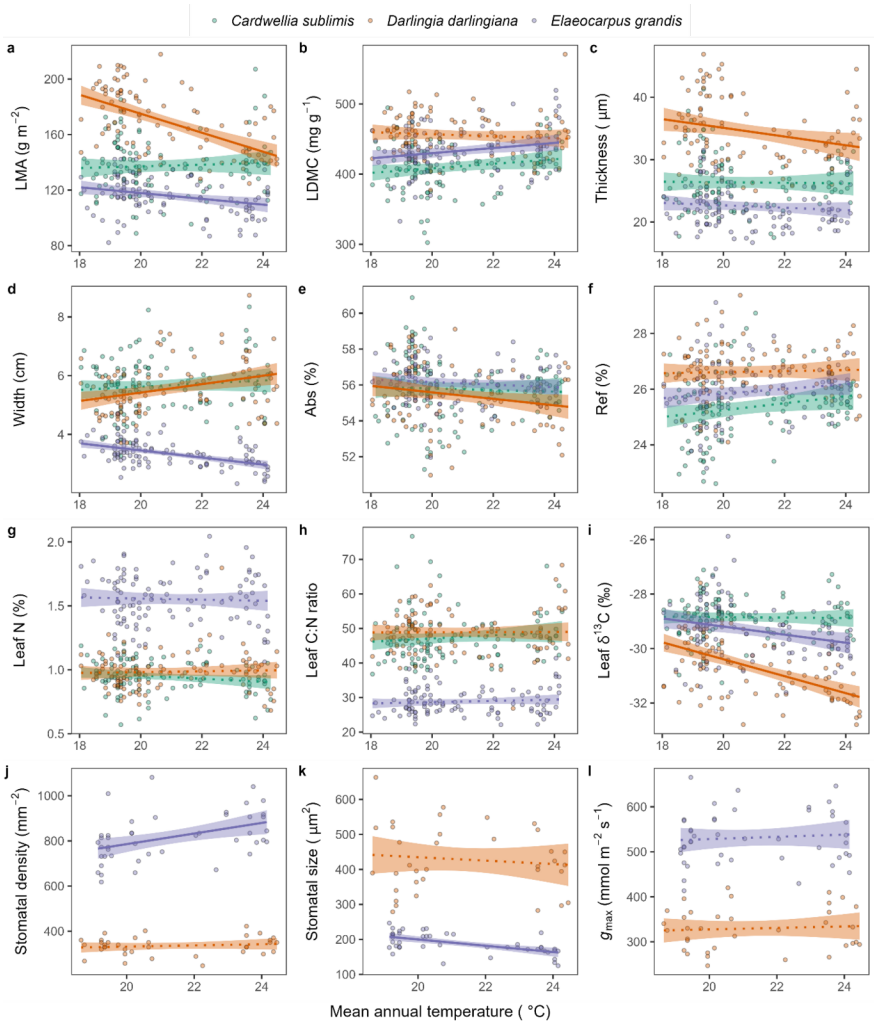

Figure S 2. Leaf trait relationships with mean annual temperature across the Wet Tropics for three tropical tree species. Each point represents an individual tree average of 10 leaves (or 3 for Abs and stomatal anatomy). Significant correlations ($P < 0.05$) are denoted by solid lines whereas nonsignificant relationships are denoted by dashed lines. Shaded regions represent standard error.

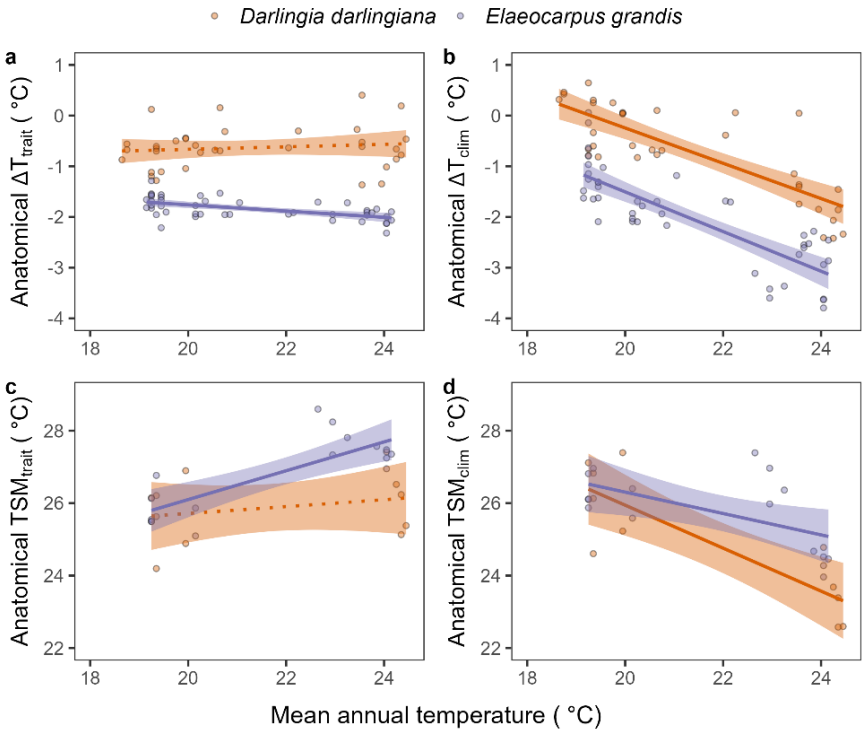

Figure S3. Variation in anatomical trait-based leaf-to-air temperature differences (anatomical [?]T; a-b), and thermal safety margins (anatomical TSM; c, d) with mean annual temperature across the distribution of*D. darlingiana* and *E. grandis* . Note in a and c [?]T is based on leaf trait variation with the same microclimate inputs for all trees, whereas in b and d, microclimate inputs also vary with each individual tree. Each point represents an individual-tree level average. Significant correlations with mean annual temperature are denoted by solid regression lines whereas non-significant correlations are dotted. Shaded region represents standard errors.

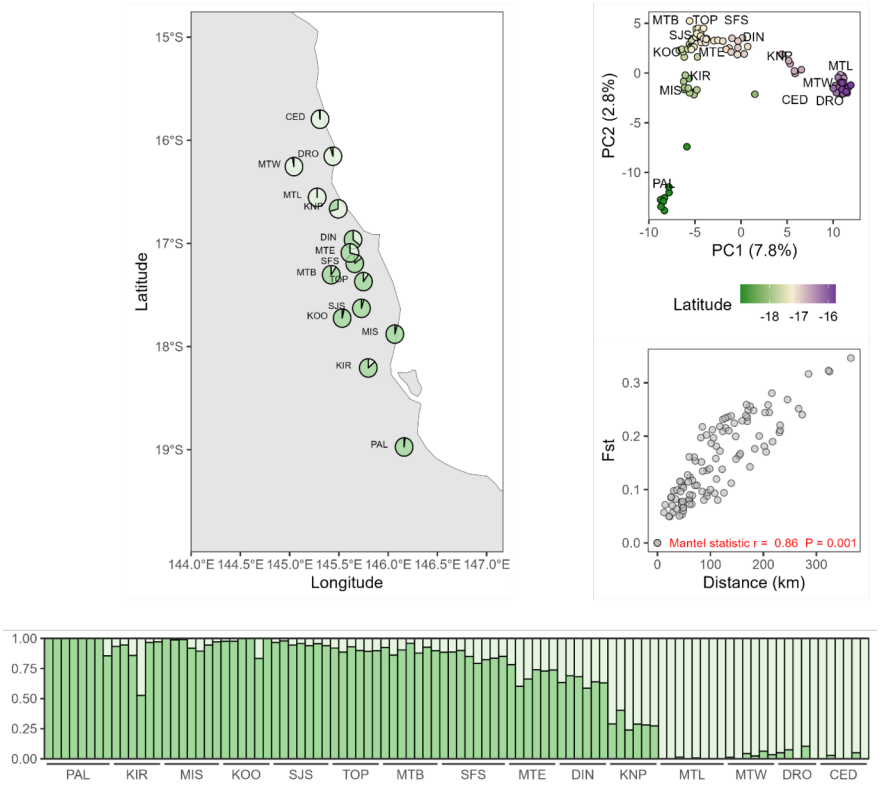

Figure S4. Population structure results for Cardwellia sublimis. Map with pie charts (top left) representing proportion of ancestry contribution corresponding to bar plot, ordered by latitude (bottom) with dark and light green colours representing the two different ancestry groups. Principal component plot (top right) shows the genetic similarity of individuals with point colours corresponding to latitude, and isolation by distance plot (centre, right)

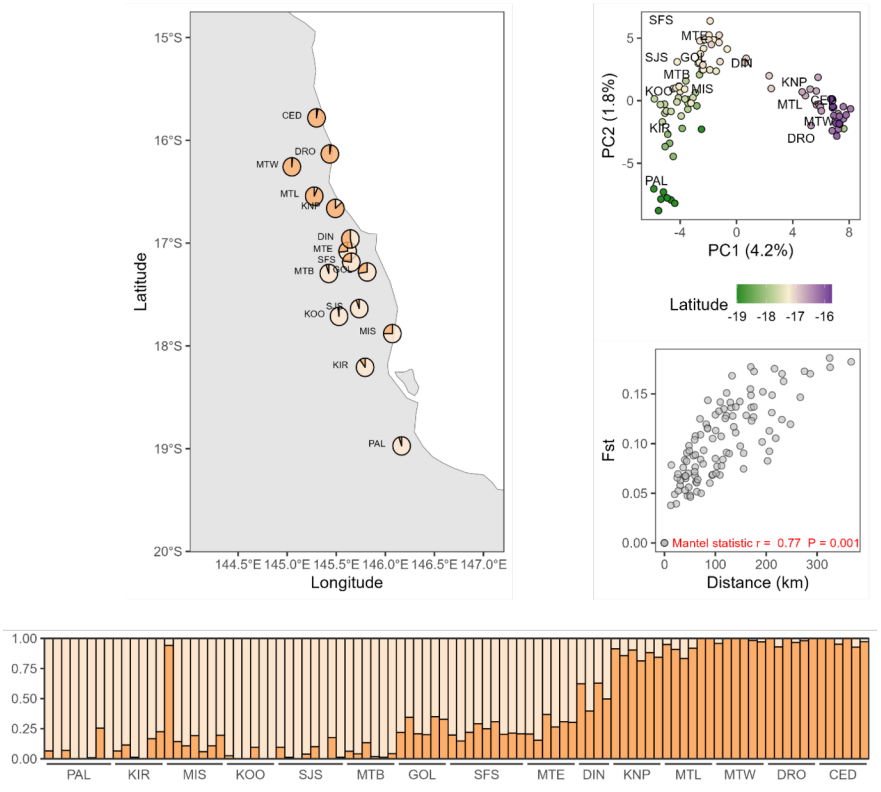

Figure S5. Population structure results for Darlingia darlingiana. Map with pie charts (top left) representing proportion of ancestry contribution corresponding to bar plot, ordered by latitude (bottom) with dark and light green colours representing the two different ancestry groups. Principal component plot (top right) shows the genetic similarity of individuals with point colours corresponding to latitude, and isolation by distance plot (centre, right).

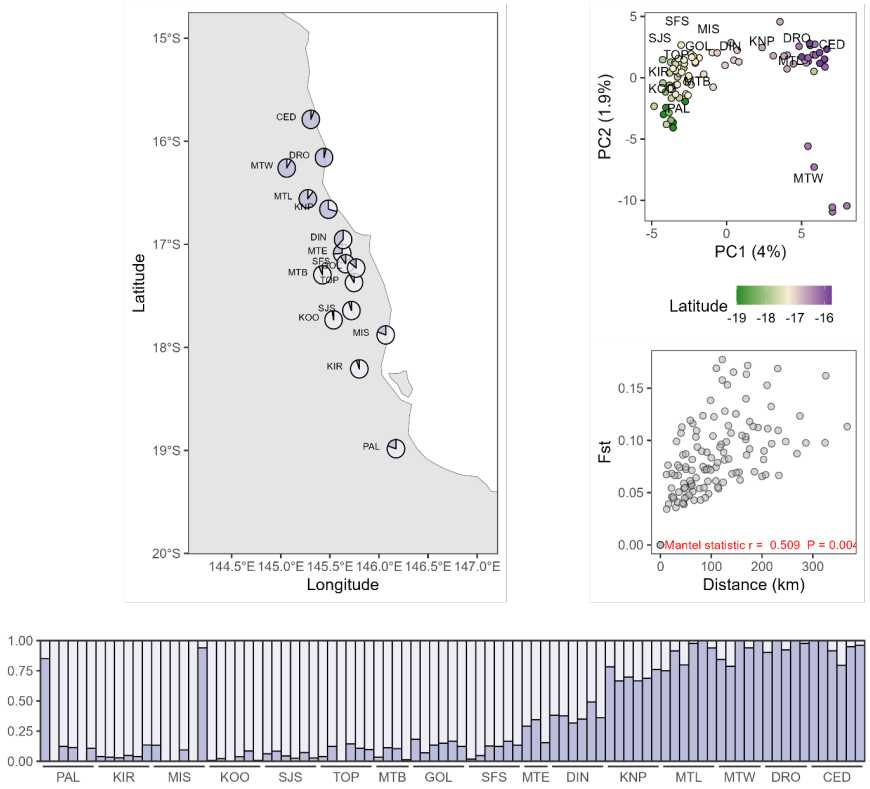

Figure S6. Population structure results for Elaeocarpus grandis. Map with pie charts (top left) representing proportion of ancestry contribution corresponding to bar plot, ordered by latitude (bottom) with dark and light green colours representing the two different ancestry groups. Principal component plot (top right) shows the genetic similarity of individuals with point colours corresponding to latitude, and isolation by distance plot (centre, right).

Table S4. Population genetic diversity metrics for each species. AR = Allelic richness, Hobs = observed Heterozygosity, Hexp = expected Heterozygosity, Fis = inbreeding coefficient.

Population	*Cardwellia sublimis*	*Darlingia darlingiana*	*Elaeocarpus grandis*		
	AR (C.I.)	**H_{obs}**	**H_{exp}**	**F_{IS} (C.I.)**	**AR**
1. Cedar Bay	1.41 (1.28, 1.49)	0.13	0.17	0.19 (0.18, 0.20)	1.36 (1.22, 1
2. Daintree	1.40 (1.24, 1.49)	0.13	0.17	0.21 (0.19, 0.22)	1.37 (1.24, 1
3. Mt Windsor	1.41 (1.26, 1.49)	0.12	0.18	0.24 (0.22, 0.25)	1.37 (1.25, 1
4. Mt Lewis	1.46 (1.38, 1.52)	0.14	0.18	0.18 (0.17, 0.19)	1.38 (1.25, 1
5. Kuranda	1.48 (1.33, 1.58)	0.16	0.19	0.13 (0.12, 0.14)	1.41 (1.26, 1
6. Dinden	1.50 (1.34, 1.59)	0.16	0.20	0.11 (0.10, 0.13)	1.37 (1.28, 1
7. Mt Edith	1.50 (1.34, 1.6)	0.16	0.20	0.15 (0.13, 0.16)	1.42 (1.24, 1
8. Danbulla	1.50 (1.39, 1.59)	0.14	0.21	0.24 (0.22, 0.25)	1.47 (1.31, 1
9. Goldsborough	NA	NA	NA	NA	1.43 (1.28, 1
10. Mt Baldy	1.48 (1.32, 1.57)	0.14	0.20	0.21 (0.20, 0.22)	1.43 (1.29, 1
11. Topaz	1.48 (1.32, 1.58)	0.15	0.20	0.20 (0.18, 0.21)	NA
12. South Johnstone	1.51 (1.43, 1.59)	0.15	0.20	0.19 (0.18, 0.20)	1.46 (1.3, 1.5
13. Tully Falls	1.46 (1.31, 1.56)	0.14	0.19	0.19 (0.18, 0.20)	1.40 (1.27, 1
14. Mission Beach	1.49 (1.35, 1.58)	0.15	0.20	0.19 (0.17, 0.20)	1.43 (1.28, 1

Population	*Cardwellia sublimis*	*Darlingia darlingiana*	*Elaeocarpus grandis*		
15. Kirrama	1.51 (1.32, 1.62)	0.17	0.21	0.13 (0.12, 0.14)	1.38 (1.21, 1
16. Paluma Range	1.42 (1.3, 1.49)	0.13	0.18	0.20 (0.19, 0.21)	1.41 (1.22, 1

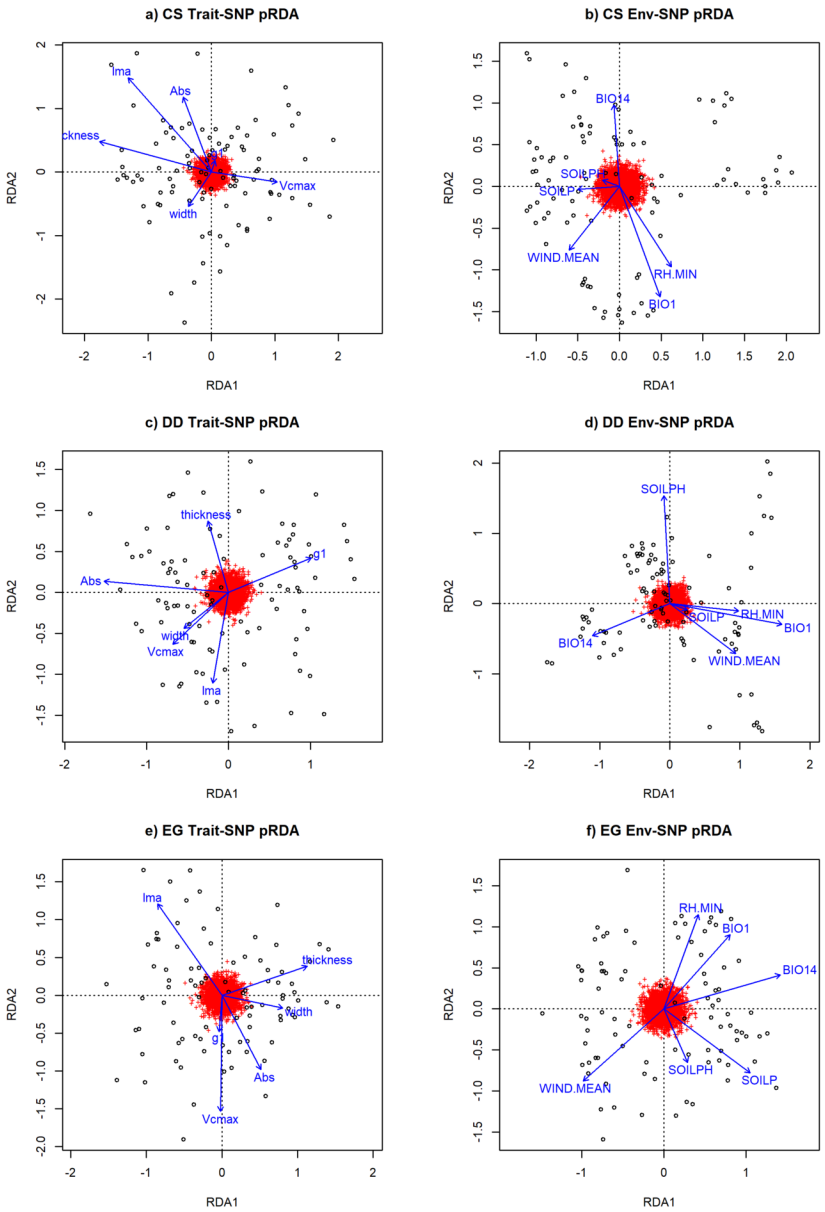

Figure S7. Partial redundancy analysis (pRDA) of genotype variation for each species. The plot displays the relationship between the SNPs with traits (a, c, e) or environment (b, d, f) along the first two RDA axes.

Table S5. Number of candidate SNPs identified by each method.

		Number of Candidate SNPs		
Analysis	Method	C. sublimis	D. darlingiana	E. grandis
GPA	[?]Ttrait LFMM	0	3	1
GPA	[?]Ttrait pRDA	63	69	45
GPA	Leaf trait LFMM	1	40	3
GPA	Leaf trait pRDA	66	63	28
GEA	Environment LFMM	13	24	1
GEA	Environment pRDA	72	63	29
Outlier	PCADAPT	243	60	126

Table S6. Generalised dissimilarity modelling results

Species	**Response variable**	**Deviance explained (%)**	**Intercept**	**Top 6 significant predictors**
Cardwellia sublimis	All SNPs	76.89	0.04	Geographic, Bio14, $Wind_{mean}$, N
	GEA & Outlier SNPs	61.93	0.07	Geographic, Bio14, RH_{min}, Soil
	GPA SNPs	66.6	0.05	Geographic, Soil pH, Bio14, Wi
	[?]T_{trait}	36.45	0.16	Soil pH, RH_{min}, MAT, Geograp
	Trait PCA	34.1	0.22	Bio14, Soil P, MAT, Soil pH, W
Darlingia darlingiana	All SNPs	68.08	0.03	Geographic, Bio14, Bio1, $Wind_r$
	GEA & Outlier SNPs	61.9	0	Geographic, MAT, Bio14, Soil p
	GPA SNPs	49.05	0.04	Geographic, MAT, Bio14, RH_{mi}
	[?]T_{trait}	44.07	0.07	MAT, Bio14, Soil pH, Geograph
	Trait PCA	21.69	0.44	Bio14, MAT, Geographic, RH_{mi}
Elaeocarpus grandis	All SNPs	65.8	0.04	Geographic, Bio14, RH_{min}, MA
	GEA & Outlier SNPs	58.98	0.01	Geographic, Bio14, MAT, RH_{mi}
	GPA SNPs	27.47	0.07	Geographic, Bio14, MAT
	[?]T_{trait}	37.27	0.07	MAT, Soil pH, RH_{min}, Geograp
	Trait PCA	20.93	0.32	MAT, RH_{min}, Geographic

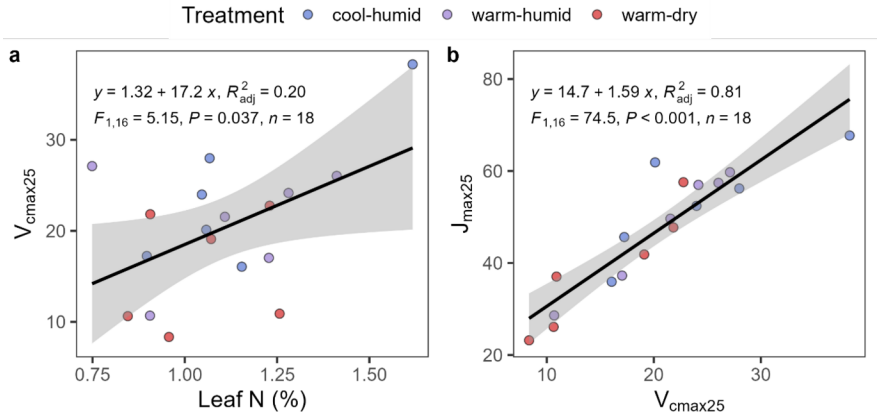

Figure S8. Correlation between photosynthetic parameters and leaf nitrogen determined in the glasshouse trial. V_{cmax25} = maximum carboxylation rate and J_{max25} = maximum rate of electron transport. Each

point represents a plant level mean. Coefficients from linear regressions used to predict V_{cmax25} and J_{max25} in the field.

Table S7. ANOVA results from *E. grandis* glasshouse trial.

Trait	**Variable**	**Chisq**	**Df**	***P* value**	**Sig**
[?]T_{trait}	MAT	11.26	1	0.0008	***
	Treatment	1.94	2	0.3793	ns
	MAT × Treatment	1.66	2	0.4362	ns
Leaf width	MAT	6.78	1	0.0092	**
	Treatment	13.55	2	0.0011	**
	MAT × Treatment	1.33	2	0.5155	ns
Log10(g_1)	MAT	5.82	1	0.0158	*
	Treatment	4.01	2	0.1347	ns
	MAT × Treatment	2.13	2	0.3451	ns
$V_{cmax.leafN}$	MAT	0.09	1	0.7617	ns
	Treatment	8.12	2	0.0173	*
	MAT × Treatment	0.77	2	0.6799	ns